Leigh syndrome associated with a mutation in the NDUFS7 (PSST) nuclear encoded subunit of complex I

Triepels, R.H.; van den Heuvel, L.P.; Loeffen, J.L.C.M.; Buskens, C.A.F.; Smeets, R.J.P.; Rubio Gozalbo, M.E.; Budde, S.M.S.; Mariman, E.C.; Wijburg, F.A.; Barth, P.G.; Trijbels, J.M.F.; Smeitink, J.A.M.

DOI
10.1002/1531-8249(199906)45:6<787::AID-ANA13>3.0.CO;2-6

Publication date
1999

Published in
Annals of Neurology

Leigh Syndrome Associated with a Mutation in the NDUFS7 (PSST) Nuclear Encoded Subunit of Complex I

R. H. Triepels, MSc,* L. P. van den Heuvel, PhD,*
J. L. C. M. Loeffen, MD,* C. A. F. Buskens, MSc,*
R. J. P. Smeets, BSc,* M. E. Rubio Gozalbo,*
S. M. S. Budde,* E. C. Mariman,†
F. A. Wijburg, MD, PhD,‡ P. G. Barth, MD, PhD,‡
J. M. F. Trijbels, PhD,* and J. A. M. Smeitink, MD, PhD*

Leigh syndrome is the phenotypical expression of a genetically heterogeneous cluster of disorders, with pyruvate dehydrogenase complex deficiency and respiratory chain disorders as the main biochemical causes. We report the first missense mutation within the nuclear encoded complex I subunit, NDUFS7, in 2 siblings with neuropathologically proven complex I–deficient Leigh syndrome.

Triepels RH, van den Heuvel LP, Loeffen JLCM, Buskens CAF, Smeets RJP, Rubio Gozalbo ME, Budde SMS, Mariman EC, Wijburg FA, Barth PG, Trijbels JMF, Smeitink JAM. Leigh syndrome associated with a mutation in the NDUFS7 (PSST) nuclear encoded subunit of complex I. Ann Neurol 1999;45:787–790

NADH:ubiquinone oxidoreductase (complex I), the largest of the four respiratory chain complexes, transfers electrons with a high redox potential from NADH to ubiquinone.[1]

Complex I deficiency is frequently encountered. Although the age at onset and course of this disease may vary, many complex I–deficient patients suffer from a progressive, often early fatal multisystem disorder,[2] frequently Leigh syndrome.[3] The genetic causes of complex I–deficient patients, in which mitochondrial DNA (mtDNA) mutations have been excluded, may be the result of mutations in the nuclear encoded complex I subunits.

To obtain more insight in the contribution of nuclear complex I genes to dysfunction of the complex, we started a mutational detection program for nuclear complex I genes in complex I–deficient patients. Nuclear genes already present in the minimal form of complex I of *Escherichia coli* and genes coding for proteins displaying a theoretically important role in the function of the complex[4] were the first to be analyzed.

The mutational detection study of the human nuclear encoded complex I subunit NDUFS7,[5] the *Nuo*B subunit counterpart of *E. coli*,[6] revealed a valine to methionine amino acid substitution that cosegregated in a neuropathologically proven Leigh syndrome family with complex I deficiency.

Patient Report

A study of a patient with complex I–deficient neuropathologically proven Leigh syndrome without lactic acidosis was published in 1991.[7] The nonconsanguineous parents were Dutch.

The second boy in this family developed, from the age of 11 months, periodic but otherwise unexplained vomiting. From the age of about 3 years, a progressive deterioration was noted. He developed left-sided hemiplegia, dysarthria and an abnormal breathing pattern with regularly deep breaths, and severe feeding difficulties requiring tube feeding. There was generalized hypotonia at rest and increased tendon reflexes. As in the case of his brother, measurements of lactate and pyruvate concentrations in urine, blood, and cerebrospinal fluid were repeatedly normal. An oral glucose loading test (2 g/kg of body weight) showed no pathological increment of lactate, pointing to a normal cytosolic redox status. A long-chain triglyceride loading test (1.5 ml/kg of body weight) revealed normal ketone body ratios, indicating a normal mitochondrial redox status.

Electroencephalogram and visual evoked potentials were normal. Brain acoustical evoked response showed a low 5th potential after right acoustic stimulation. Brain magnetic resonance imaging showed bilateral putaminal, caudate, and dentate lesions, and lesions of the left cerebral peduncle and right paramedian area of the medulla oblongata with enhanced T2 signal. The patient died at 5 years of age.

Patients and Methods

Patient Investigations

Our patient study group consists of 20 children with isolated decreased biochemical complex I activity in skeletal muscle tissue and cultured skin fibroblasts.[8–10]

To exclude large mtDNA rearrangements, we analyzed the entire mitochondrial genome with a previously developed long template polymerase chain reaction (PCR) technique.[11] We screened the mitochondrial genome of the patients for the mtDNA mutations T14484C, G14459A, G11778A, T4160C, G3460A, T8993G/C, T8356C, A8344G, A4317G, T3271C, and A3243G. On the nuclear level, mutational detection of patient fibroblast cDNA of other possi-

From the *Nijmegen Center for Mitochondrial Disorders, Department of Pediatrics, University Children's Hospital, and †Department of Human Genetics, University Hospital Nijmegen, Nijmegen; and ‡Department of Pediatrics, Academic Medical Center, University of Amsterdam, Amsterdam, The Netherlands.

Received Oct 7, 1998, and in revised form Jan 25, 1999. Accepted for publication Jan 25, 1999.

Address correspondence to Dr van den Heuvel, Nijmegen Center for Mitochondrial Disorders, Department of Pediatrics, University Children's Hospital Nijmegen, Geert Grooteplein 20, PO Box 9101, 6500 HB Nijmegen, The Netherlands.

ble candidate genes (NDUFA1, NDUFB6, NDUFS4, NDUFS5, and NDUFS8) was performed by direct DNA sequencing.

Mutational Detection in the NDUFS7 cDNA

Mutational detection was performed as described previously.[12] For PCR amplification of the human NDUFS7[5] cDNA, the forward primer as well as the reverse primer (Table 1), homologous to the 5′ and 3′ untranslated regions, were designed according to human EST (Expressed Sequence Tags),[13] and interior primers were ordered according to the published NDUFS7 cDNA sequence.

Tissue Distribution of NDUFS7 mRNA

To obtain more information concerning mRNA quantities of the human NDUFS7 in a wide range of human tissues, we used a human poly(A)$^+$ RNA Master Blot (Clontech, Madison, WI). Hybridization was performed according to established procedures by using [α-^{32}P]dCTP-labeled wild-type cDNA PCR fragment containing the NDUFS7 open reading frame.[10] Afterward the blot was analyzed by autoradiography.

Results

Genetic Analysis of the Patient Group

Amplification of the entire mitochondrial genome of all patients showed no large mtDNA deletions or insertions. None of the investigated mtDNA abnormalities were detected. Two mutations in nuclear encoded complex I subunits were found, a 5-bp duplication in the NDUFS4 subunit in a non-Leigh syndrome complex I–deficient patient[12] and a compound heterozygous mutation in the NDUFS8 gene within another neuropathologically proven Leigh syndrome family.[14]

Biochemical Analysis of Index Patients

Biochemical studies (Table 2) revealed a complex I deficiency in muscle tissue of both affected siblings. Individual NADH:QI oxidoreductase (complex I) activities as well as complex I/citrate synthase and complex I/cytochrome *c* oxidase ratios were decreased compared with representative reference values. In cultured fibroblasts, a decreased complex I activity and complex I/cytochrome *c* oxidase ratio were detected in Sibling 2.

Mutational Detection of the NDUFS7 cDNA

For mutational detection of the NDUFS7, we analyzed patient cDNA, produced by first-strand synthesis of cultured fibroblast RNA. By using the oligonucleotide primers *NDUFS7-F* and *R* (see Table 1), we amplified a 775-bp cDNA PCR fragment containing the complete NDUFS7 open reading frame. Direct sequencing of the obtained fragment revealed a homozygous *G364A* transition in 1 patient (Sibling 2), which results in a V122M amino acid substitution. The *G364A* transition creates a *Bcl*I restriction site. Analysis of cDNA produced by first-strand synthesis of RNA of both parents and a younger affected brother (Sibling 1) revealed that this mutations is consistent with an autosomal recessive mode of inheritance (Fig). The *G364A* mutation was not present in 60 Dutch control alleles and another 19 complex I–deficient patients, including 5 patients displaying the clinical phenotype of Leigh syndrome.

In addition, a *T68C* transition, introducing a *Msp*I restriction site on the DNA level and a *L23P* amino acid substitution on the protein level, was observed. *Msp*I restriction analysis revealed an allelic frequency of this transition of 37.5% in 19 isolated complex I–deficient patients and 35% in 60 control alleles.

Tissue Distribution of NDUFS7 Transcripts

In descending order, the ubiquitously expressed NDUFS7 mRNA was extensively detected in human heart, skeletal muscle, and liver (data not shown). In comparison with other tissues, the NDUFS7 mRNA content in pancreas, adrenal gland, salivary gland, and stomach seems to be slightly more.

Discussion

Complex I deficiency is a frequent mitochondrial respiratory chain defect with Leigh syndrome as a common clinical phenotype.[15] In the past decade, several mitochondrial mutations were associated with complex I deficiency (reviewed by Zeviani and colleagues[16]). The transfer of electrons through complex I is possible

Table 1. Human NDUFS7 cDNA Primer Sequences Used for cDNA Sequencing and Mutational Detection

Primer Names	Oligonucleotide Sequences	Positions on cDNA
Forward primers		
NDUFS7-F	5′-CTG AAG GCC GAG GCC AAG-3′	−1/−18
NDUFS7-F1	5′-GTT CTC TGT GGC CCA TGA CC-3′	230/249
NDUFS7-F2	5′-CTA TTC CTA CTC GGT GGT G-3′	483/501
Reverse primers		
NDUFS7-R	5′-CCT CAC GGG ACA CAA GCA G-3′	757/739
NDUFS7-R1	5′-CCG AGT AGG AAT AGT GGT AG-3′	496/477
NDUFS7-R2	5′-GTT GAC GAG GTC ATC CAG C-3′	216/198

The NDUFS7 open reading frame contains 640 base pairs to the first base of the TAG stop codon.[5]

Table 2. Enzyme Activities in Skeletal Muscle and Fibroblasts

	Enzyme Activities					
	Skeletal Muscle Tissue			Cultured Fibroblasts		
Parameter Analyzed	Sibling 1	Sibling 2	Control	Sibling 1	Sibling 2	Control
NADH:Q1 oxidoreductase (CI)	0.7[a]	2.8[a]	3.6–25[a] (n = 20)	NA	13.6[a]	18.9–44.2[a] (n = 14)
Cytochrome *c* oxidase (COX)	1,500[b]	1,488[b]	810–3,120[b] (n = 21)	NA	201[a]	143–252[a] (n = 14)
Citrate synthase (CS)	36[a]	172[a]	37–162[a] (n = 43)	NM	NM	NM
CI/CS	19.4[b]	16.3[b]	70–190[b] (n = 20)	NM	NM	NM
CI/COX	13.0[c]	10.9[c]	38–164[c] (n = 20)	NA	68[c]	110–260[c] (n = 14)

[a]Values are expressed as milliunits per milligram of protein.
[b]Values are expressed as milliunits per units of CS.
[c]Values are expressed as milliunits per units of COX.

NA = not available; NM = not measurable.

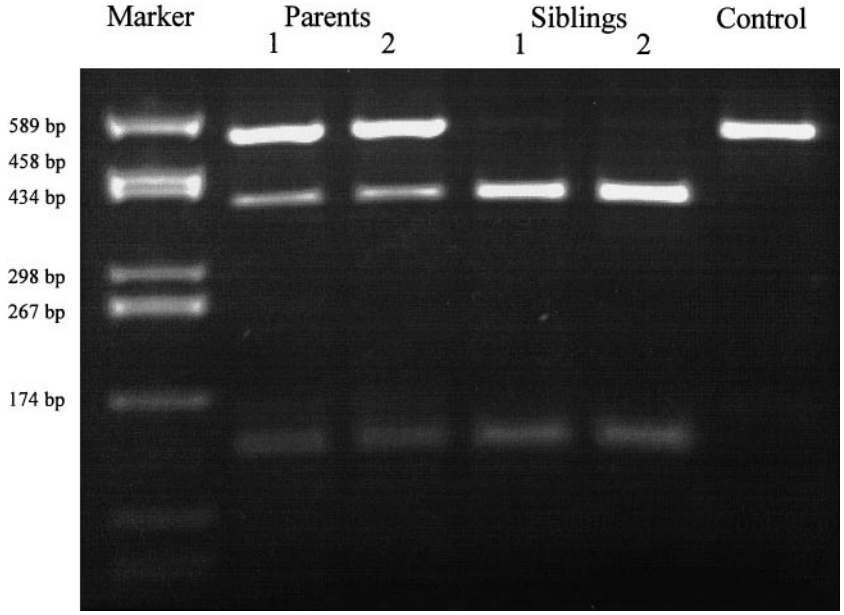

Fig. Segegration of the NDUFS7 V122M mutation within the family. Genetic analysis was performed by BclI *restriction analysis (see Results). The presence of the G364A transition results in the digestion of the 514-bp polymerase chain reaction fragment into 377-bp and 137-bp fragments. On the cDNA level, both parents appear to be heterozygous for the G364A transition, whereas both affected siblings are homozygous.*

through the presence of a flavin mononucleotide center and at least six iron–sulfur clusters.[17,18] Complex I deficiency might be caused by defects of subunits involved in the formation of these clusters. The human nuclear encoded NDUFS7 protein seems to be a strong candidate to be involved in the formation of the N2 (4Fe-4S) iron–sulfur cluster.[19]

Mutational detection of the NDUFS7 cDNA in the described complex I–deficient Leigh syndrome family revealed a valine to methionine (V122M) amino acid substitution consistent with an autosomal recessive mode of inheritance (see Fig). The substituted valine is located within the NDUFS7 cysteine motif —CxxE—$(x)_{60}$—C—$(x)_{30}$—CP—,[5] which is probably involved in the formation of the N2 (4Fe-4S) iron–sulfur cluster of complex I.[17] The V122M amino acid substitution could affect the NDUFS7 protein conformation in complex I or its incorporation in the whole complex, thus impairing for the proper formation of the iron–-sulfur cluster. Protein sequence conservation among various organisms such as *Bos taurus*, *Caenorhabditis elegans*, *Neurospora crassa*, *Escherichia coli*, and *Rhodobacter capsulatus* shows a high conservation rate of the substituted valine residue, suggesting an important role in complex I. The NDUFS7 cDNA analysis revealed also a leucine to proline substitution (*L23P*) with a comparable distribution in complex I–deficient patients and a control population.

NDUFS7 transcripts were found in all human tissues, indicating a NDUFS7 expression pattern like housekeeping genes. The higher expression in human tissues with high metabolic energy rates is probably caused by higher amounts of mitochondria in these tissues.

The appearance of a mutation within the nuclear encoded subunit NDUFS7 of complex I in 2 siblings displaying Leigh syndrome links this disease in this family to a nuclear defect. Although frequently present, it is important to stress that normal concentrations of lactate, pyruvate, and ketone body ratios in body fluids as well as normal magnetic resonance spectroscopy results do not definitely rule out mitochondrial disorders.

The functional relevance of mutations in the nuclear encoded subunits in complex I deficiency should be tested in the future, to yield insight into the pathogenetic mechanism involved. This information might prove useful, because treatment of these disorders is difficult.

This study was funded by a grant from the "Prinses Beatrix Fonds (97-0111)," The Netherlands.

We greatly appreciate Grazia Mauceri and Antoon Janssen for measurement of the complex I activity in cultured skin fibroblasts, Melan Bakker for mtDNA analyses, and Rob Sengers for continuous support.

References

1. Walker JE. The NADH:ubiquinone oxidoreductase (complex I) of respiratory chains. Q Rev Biophys 1992;25:253–324
2. Pitkanen S, Feigenbaum A, Laframboise R, Robinson BH. NADH-coenzyme Q reductase (complex I) deficiency: heterogeneity in phenotype and biochemical findings. J Inherit Metab Dis 1996;19:675–686
3. Rahman S, Blok RB, Dahl HH, et al. Leigh syndrome: clinical features and biochemical and DNA abnormalities. Ann Neurol 1996;39:343–351
4. Smeitink JAM, Loeffen JLCM, Triepels RH, et al. Nuclear genes of human complex I of the mitochondrial electron transport chain: state of the art. Hum Mol Genet 1998;7:1573–1579
5. Hyslop SJ, Duncan AM, Pitkanen S, Robinson BH. Assignment of the PSST subunit gene of human mitochondrial complex I to chromosome 19p13. Genomics 1996;37:375–380
6. Weidner U, Geier S, Ptock A, et al. The gene locus of the proton-translocating NADH:ubiquinone oxidoreductase in *Escherichia coli*: organization of the 14 genes and relationship between the derived proteins and subunits of mitochondrial complex I. J Mol Biol 1993;233:109–122
7. Wijburg FA, Wanders RJ, van Lie-Peters EM, et al. NADH:Q1 oxidoreductase deficiency without lactic acidosis in a patient with Leigh syndrome: implications for the diagnosis of inborn errors of the respiratory chain. J Inherit Metab Dis 1991;14:297–300
8. Fischer JC, Ruitenbeek W, Trijbels JM, et al. Estimation of NADH oxidation in human skeletal muscle mitochondria. Clin Chim Acta 1986;155:263–273
9. Bentlage HA, Wendel U, Schägger H, et al. Lethal infantile mitochondrial disease with isolated complex I deficiency in fibroblasts but with combined complex I and IV deficiencies in muscle. Neurology 1996;47:243–248
10. Loeffen J, Smeets R, Smeitink J, et al. The X-chromosomal NDUFA1 gene of complex I in mitochondrial encephalomyopathies: tissue expression and mutation detection. J Inherit Metab Dis 1998;21:210–215
11. Li YY, Hengstenberg C, Maisch B. Whole mitochondrial genome amplification reveals basal level multiple deletions in mtDNA of patients with dilated cardiomyopathy. Biochem Biophys Res Commun 1995;210:211–218
12. van den Heuvel L, Ruitenbeek W, Smeets R, et al. Demonstration of a new pathogenic mutation in human complex I deficiency: a 5-bp duplication in the nuclear gene encoding the 18-kD (AQDQ) subunit. Am J Hum Genet 1998;62:262–268
13. Adams MD, Kelley JM, Gocayne JD, et al. Complementary DNA sequencing: expressed sequence tags and human genome project. Science 1991;252:1651–1656
14. Loeffen JLCM, Smeitink JAM, Triepels RH, et al. The first nuclear encoded complex I mutation in a patient with Leigh syndrome. Am J Hum Genet 1998;63:1598–1608
15. Robinson BH. Human complex I deficiency: clinical spectrum and involvement of oxygen free radicals in the pathogenicity of the defect. Biochim Biophys Acta 1998;1364:271–286
16. Zeviani M, Tiranti V, Piantadosi C. Mitochondrial disorders. Medicine (Balt) 1998;77:59–72
17. Ohnishi T. Iron-sulfur clusters/semiquinones in complex I. Biochim Biophys Acta 1998;1364:186–206
18. Albracht SP, Mariette A, de Jong P. Bovine-heart NADH: ubiquinone oxidoreductase is a monomer with 8 Fe-S clusters and 2 FMN groups. Biochim Biophys Acta 1997;1318:92–106
19. Ohnishi T, Ragan CI, Hatefi Y. EPR studies of iron-sulfur clusters in isolated subunits and subfractions of NADH-ubiquinone oxidoreductase. J Biol Chem 1985;260:2782–2788

Chromatic Sensitive Epilepsy: A Variant of Photosensitive Epilepsy

Shozo Tobimatsu, MD,* You Min Zhang, MD,* Yasuko Tomoda, MD,† Akihisa Mitsudome, MD,† and Motohiro Kato, MD*

We herein report 4 Japanese children who suffered epileptic seizures while watching a popular animated TV program. They showed a photoparoxysmal response that is more frequently observed in response to rapid color (blue/red) frame changes than monochromatic ones. These patients were all considered to have photosensitive epilepsy; however, chromatic sensitivity also plays an important role in the generation of such seizures.

Tobimatsu S, Zhang YM, Tomoda Y, Mitsudome A, Kato M. Chromatic sensitive epilepsy: a variant of photosensitive epilepsy. Ann Neurol 1999;45:790–793

From the *Department of Clinical Neurophysiology, Neurological Institute, Faculty of Medicine, Kyushu University, and †Department of Pediatrics, Faculty of Medicine, Fukuoka University, Fukuoka, Japan.

Received Nov 11, 1998, and in revised form Jan 26, 1999. Accepted for publication Jan 26, 1999.

Address correspondence to Dr Tobimatsu, Department of Clinical Neurophysiology, Neurological Institute, Faculty of Medicine, Kyushu University, 3-1-1 Maidashi, Higashi-Ku, Fukuoka 812-8582, Japan.

Photosensitive epilepsy (PSE) occurs in approximately 1 of 4,000 individuals from the general population and tends to be most prevalent in adolescence.[1] PSE can be caused by flickering light or high-contrast patterned stimuli. PSE patients usually show a photoparoxysmal response (PPR) to intermittent photic stimulation (IPS) in electroencephalography (EEG).

On December 16, 1997, at around 18:50 PM, 685 Japanese children and some adults suffered generalized convulsions and a loss of consciousness suggesting epileptic seizures, while watching a popular animated TV program called "Pocket Monsters."[2–4] The probable cause was PSE because a tremendous number of children developed similar symptoms at exactly the same time in a similar situation when watching a scene consisting of flashing lights and rapid color changes in the cartoon. However, it is not clear as to why many children without any previous seizures were also affected or exactly which components of the cartoon constituted the provocative stimuli. Therefore, a research committee was organized by the Ministry of Welfare and Health of the Japanese Government.[2] As members of this committee, we conducted research on these patients. We herein report the evidence that rapid changes of red and blue color frames were found to be the provoking factor for these seizures.

Patients and Methods

Twenty children (11 boys and 9 girls; age, 5–17 years) with seizures provoked by a cartoon that was broadcast on December 16, 1997, were referred to the Department of Pediatrics of Fukuoka University.[2] Four boys (age, 8–13 years) were recruited from these 20 cases for further investigation (Table). Patient 4 had been taking sodium valproate because a referred pediatrician found a PPR in his EEG. Two boys with TV game epilepsy (ages 11 and 14 years) also participated in this investigation. They did not have seizures while watching the cartoon. A 14-year-old boy was the older brother of Patient 4 (see Table) and had been receiving sodium valproate. Informed consent was obtained from all subjects and their parents after the procedure had been fully explained.

All patients underwent a comprehensive EEG investigation including hyperventilation. IPS was performed by using a photostimulator (NEC San-ei or Nihon Kohden, Tokyo, Japan) at a distance of 30 cm from the patient's eyes. In addition, EEG recordings were made while watching the critical sequences of the cartoon that had induced seizures. The patient sat 1.3 m from the video monitor, which subtended a visual angle of 23.1° horizontally and 17.4° vertically. We also presented rapid changes of blue and red (B/R) color frames and monochromatic gray and black (G/B) frames with varying stimulus frequencies (3, 6, 8.6, 10, 12, and 15 Hz) in 2 patients, because the committee had revealed that the background of the colored cartoon frames consisted of rapid changes of red and blue frames at 12 Hz.[2] The mean luminances of red, blue, gray, and black were 120, 160, 160, and 20 cd/m^2, respectively.

Results

All 4 boys with cartoon-evoked seizures had no previous history of afebrile convulsions before this episode, but Patient 2 had experienced febrile convulsions at 3 years of age (see Table). Two patients (Patients 2 and 4) had a family history of epilepsy and they were the only cases with a positive family history in 20 cases. Brain computed tomographic scanning or magnetic resonance imaging showed no evidence of any focal abnormality. Two patients (Patients 1 and 2) showed normal EEG findings and were not sensitive to IPS. However, the other 2 patients (Patients 3 and 4) were sensitive to IPS and showed paroxysmal EEG abnormalities.

All 4 boys with cartoon-evoked seizures had a PPR (ie, bursts of 3-Hz spike-and-wave complex) when exposed to the colored cartoon frames, but PPRs were

Table. Demographic Characteristics of the Patients and Electroencephalographic Findings

	Patient 1 (T.S.)	Patient 2 (N.T.)	Patient 3 (T.A.)	Patient 4 (M.Y.)
Age (yr)	12	8	11	13
Sex	M	M	M	M
Seizure type	GTC	GTC	GTC	GTC
Visual symptom	None	None	None	None
Febrile convulsion	None	Once (at 3 yr)	None	None
Family history	None	Present[a]	None	Present[b]
CT or MRI	N	N	N	N
EEG findings				
Awake	N	N	GSW	N
HV	N	N	GSW	Spike at C
IPS	N	N	GSW (9 Hz)	GSW (24 Hz)

GTC = generalized tonic or tonic–clonic convulsion; CT = computed tomography; MRI = magnetic resonance imaging; N = normal; EEG = electroencephalographic; HV = hyperventilation; IPS = intermittent photic stimulation; GSW = generalized (ir)regular, spike and waves, or polyspike and waves; C = central region.

[a]A younger sister has partial epilepsy with photosensitivity and an older brother has partial epilepsy without photosensitivity.
[b]An older brother has TV game epilepsy.

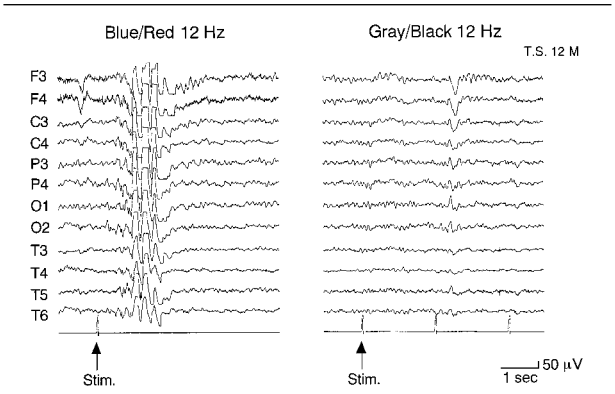

Fig 1. The photoparoxysmal response (PPR) induced by the cartoon frames (blue/red) and monochromatic version (gray/black) of the same cartoon in Patient 1. This patient was more sensitive to chromatic changes than monochromatic changes. Each stimulus was presented for 1 second.

less frequent while watching a monochromatic version of the same cartoon (Figs 1 and 2). In contrast, 2 boys with TV game epilepsy did not show a PPR when exposed to either the colored cartoon frames or monochromatic ones.

The effect of the stimulus frequency on the EEG is shown in Figure 2. This patient (Patient 2) showed a PPR to B/R color stimulus at 6 Hz and at 12 Hz, but he did not show the PPR to G/B stimuli up to 12 Hz (see Fig 2). The other patient (Patient 3) showed a PPR to B/R color stimulus at 10 Hz, but he did not show a PPR to G/B stimuli up to 12 Hz (data not shown).

Discussion

Four patients without any previous history of seizures were more sensitive to rapid color changes than to monochromatic ones. In a similar manner, 5 of 6 British PSE patients produced a PPR after viewing the colored cartoon frames but not after seeing the monochromatic ones.[5] We also found that B/R stimuli provoked a PPR even at a lower stimulus frequency when compared with achromatic ones. These findings suggest that the rapid color changes in the cartoon thus provoked the seizures. Long wavelength red light (such as that from the red frame) stimulates red cones and short wavelength blue light stimulates blue cones. It is postulated that no antagonistic relation exists between the red and blue cone impulses in the visual cortical neurons.[6] No matching inhibitory signals are elicited by stimulation with the two colors, which thus results in the maximal stimulation of the visual cortex, and

Fig 2. The effect of stimulus frequency on photoparoxysmal response (PPR) in Patient 2. Note that not only blue/red (B/R) chromatic changes at a rate of 12 Hz but also those at 6 Hz provoked a PPR. In contrast, a gray/black (G/B) flicker induced a PPR only at 12 Hz.

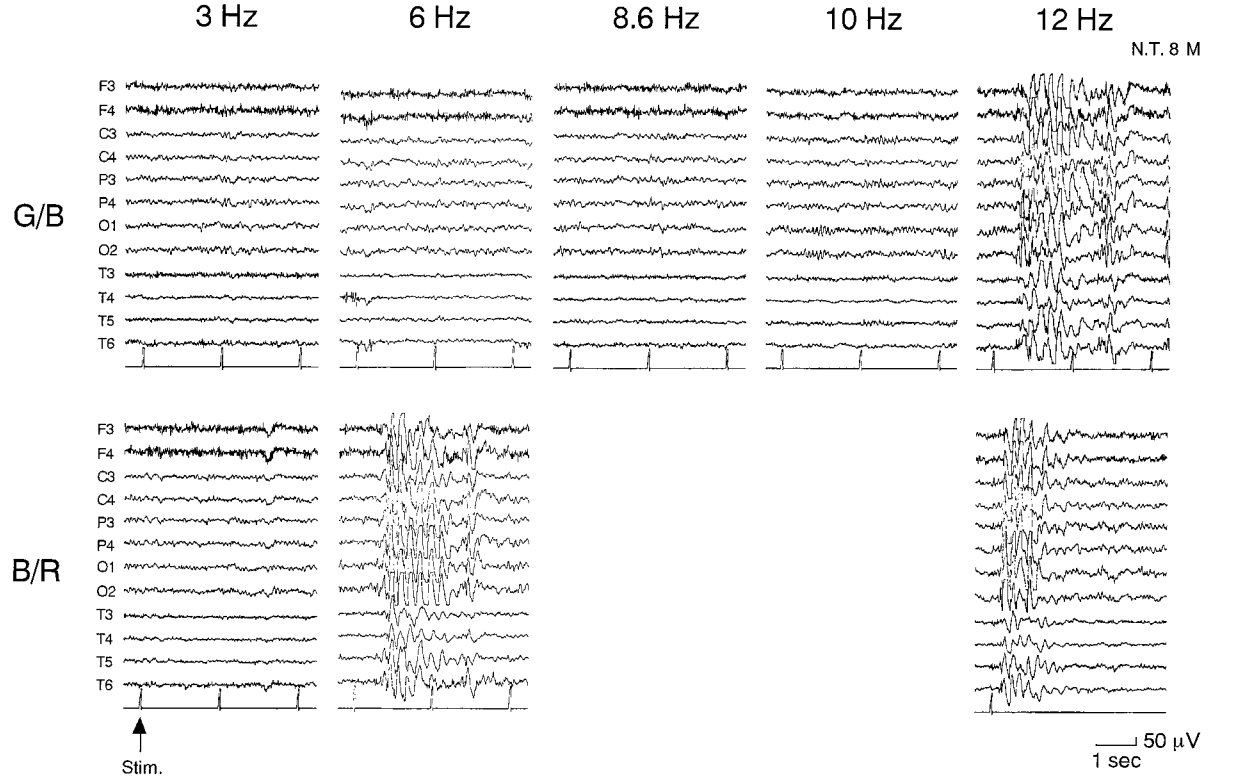

seizures in photosensitive individuals. It remains controversial, however, as to whether red light is more provocative than white light.[5,7–10] Takahashi and Tsukahara[7,8] claimed that red flickering light was more epileptogenic than white or other colors, whereas the other studies found that no consistent difference existed between red and green stimuli.[9,10] The above findings suggest that a combination of colors without any antagonistic relation in the visual cortex such as red and blue is apparently more provocative than red only.

We would like to revise the overall concept of PSE based on our findings. We propose that the following four factors play an important role in the generation of PSE: (1) photosensitivity, (2) pattern sensitivity, (3) chromatic sensitivity, and (4) stimulus frequency. Photosensitivity to IPS is well known to be essential for diagnosing PSE.[10–12] Pattern sensitivity is already known to play an important role in TV game epilepsy.[1,13,14] High-contrast black and white square-wave grating patterns at spatial frequencies between 0.5 and 6 cycles per degree are recommended for laboratory tests of pattern sensitivity.[1] Chromatic sensitivity as observed in this study is also important, especially a combination of colors without any antagonistic relation in the visual cortex such as red and blue. Finally, stimulus frequency is another important factor. PSE patients are most sensitive to the frequency range 10 to 30 Hz of IPS.[1] In a similar manner, PPRs were highly dependent on the stimulus frequency of B/R or G/B in the present study. Taken together, investigators should thus recognize that each PSE patient demonstrates a different susceptibility to these four factors. These findings suggest that testing for chromatic sensitivity as well as IPS during routine EEGs is thus required when physicians suspect chromatic sensitivity in patients.

There is a relatively high incidence of family history of epilepsy in PSE patients and about 50% of the purely photosensitive patients had a family history of photosensitivity.[15] In this study, we also found a family history positive for epilepsy, thus suggesting the genetic background underlying this chromatic sensitive condition.[2] Further studies are necessary to find the gene abnormality responsible for photosensitivity or chromatic sensitivity.

To date, our patients have not had any further attacks and we have not administered anticonvulsants for prophylaxis. However, we have recommended that the patients and their families avoid rapid changes in color, luminance, and patterns including TV and video games.[2]

In conclusion, our patients were all considered to have PSE. However, chromatic sensitivity also plays an important role in the generation of seizures. Therefore, we propose that chromatic sensitive epilepsy should be considered a variant of PSE and it appears to include a substantial population among children.

This study was supported by the Research Committee of "Clinical Research on Photosensitive Attack" of the Ministry of Welfare and Health of the Japanese Government.

References

1. Harding GFA, Jeavons PM, Edson AS. Video material and epilepsy. Epilepsia 1994;35:1208–1216
2. Yamauchi T, Ebata K, Kuroiwa Y, et al. Clinical research on photosensitive attacks. Report of a research committee of the Ministry of Welfare and Health of the Japanese Government, 1998
3. Hayashi T, Ichiyama T, Nishikawa M, et al. Pocket monsters, a popular television cartoon, attacks Japanese children. Ann Neurol 1998;44:427–428
4. Yamashita Y, Matsuishi T, Ishida S, et al. Pocket monsters attacks Japanese children via media. Ann Neurol 1998;44:428
5. Harding GFA. TV can be bad for your health. Nat Med 1998; 4:265–267 (Letter)
6. Livingstone MS, Hubel DH. Anatomy and physiology of a color system in the primate visual cortex. J Neurosci 1984;4: 309–356
7. Takahashi T, Tsukahara Y. Influence of color on the photoconvulsive response. Electroencephalogr Clin Neurophysiol 1976; 41:124–136
8. Takahashi T, Tsukahara Y. Usefulness of blue sunglasses in photosensitive epilepsy. Epilepsia 1992;33:517–521
9. Binnie CD, Estevez O, Kasteleijn-Nolst Trenité DGA, Peters A. Colour and photosensitive epilepsy. Electroencephalogr Clin Neurophysiol 1984;58:387–391
10. Harding GFA, Pearce K, Dimitrakoudi M, Jeavons PM. The effect of coloured intermittent photic stimulation (IPS) on the photoconvulsive response (PCR). Electroencephalogr Clin Neurophysiol 1975;39:428 (Abstract)
11. Panayiotopoulos CP, Jeavons PM, Harding GFA. Occipital spikes and their relation to visual evoked responses in epilepsy, with particular reference to photosensitive epilepsy. Electroencephalogr Clin Neurophysiol 1972;32:179–190
12. Jeavons PM, Harding GFA, Panayiotopoulos CP, Drasdo N. The effect of geometric patterns combined with intermittent photic stimulation in photosensitive epilepsy. Electroencephalogr Clin Neurophysiol 1972;33:221–224
13. Wilkins AJ, Darby CE, Binnie CD, et al. Television epilepsy–the role of pattern. Electroencephalogr Clin Neurophysiol 1979;47:163–171
14. Fylan F, Harding GFA. The effect of television frame rate on EEG abnormalities in photosensitive and pattern-sensitive epilepsy. Epilepsia 1997;38:1124–1131
15. Harding GFA, Edson A, Jeavons PM. Persistence of photosensitivity. Eilepsia 1997;38:663–669

Diffusion-Weighted Magnetic Resonance Imaging: Detection of Ischemic Injury 39 Minutes after Onset in a Stroke Patient

Yukihiro Yoneda, MD,* Keisuke Tokui, MD,*
Tokiji Hanihara, MD,† Hajime Kitagaki, MD,‡
Masayasu Tabuchi, MD,* and Etsuro Mori, MD†

A neurologist witnessed the in-hospital onset of an ischemic stroke in a 71-year-old right-handed male who suddenly developed global aphasia and right hemiplegia. Diffusion-weighted magnetic resonance imaging (DWI) 39 minutes after the ictus demonstrated high signals in the left internal carotid artery territory. T1- and T2-weighted images failed to detect this change. Magnetic resonance angiography showed occlusions in branches of the left anterior and middle cerebral arteries and an atheromatous stenotic lesion in the ipsilateral proximal internal carotid artery. The patient was treated with intravenous heparin and low molecular dextran solution. Repeated magnetic resonance imagings identified an infarction slightly smaller than the abnormality demonstrated by the initial DWI. DWI detects hyperacute ischemic injury within 1 hour of symptom onset in human ischemic stroke.

Yoneda Y, Tokui K, Hanihara T, Kitagaki H, Tabuchi M, Mori E. Diffusion-weighted magnetic resonance imaging: detection of ischemic injury 39 minutes after onset in a stroke patient. Ann Neurol 1999;45:794–797

Diffusion-weighted imaging (DWI) with a new functional magnetic resonance (MR) technique is very sensitive for early cerebral ischemia within the first few hours after stroke onset.[1–8] In experimental stroke models, the DWI detects focal ischemia within minutes after cerebral arterial occlusion.[9–12] In human acute ischemic stroke, however, there was little chance to obtain MR imagings including DWI within 1 hour of stroke onset.[8] We here report an ischemic stroke patient whose stroke onset was witnessed by a neurologist, in which a hyperacute ischemic injury was demonstrated by the DWI 39 minutes after the onset. This is the first documentation of experiment-based phenomenon in human hyperacute ischemic stroke.

From the *Neurology Service, Hyogo Brain and Heart Center at Himeji, and Divisions of †Clinical Neurosciences and ‡Neuroimaging Research, Hyogo Institute for Aging Brain and Cognitive Disorders, Himeji, Japan.

Received Aug 4, 1998, and in revised form Jan 29, 1999. Accepted for publication Jan 30, 1999.

Address correspondence to Dr Yoneda, Neurology Service, Hyogo Brain and Heart Center at Himeji, 520 Saisho-ko, Himeji, 670-0981, Japan.

Case Report

A 71-year-old right-handed male suddenly became mute and right hemiplegic at 10:45 AM (onset time) on May 27, 1998, while he and his wife were meeting with a neurologist (T.H.) about her medical condition (Alzheimer's disease) at the outpatient clinic of the Hyogo Institute for Aging Brain and Cognitive Disorder. His medical history was unremarkable except for left lung lobectomy for tuberculosis. Until then, he had no episodes of stroke and transient ischemic attack, and the neurologist did not notice any evidence of cognitive and neurological abnormality during the meeting with him. A brief physical and neurological examination revealed global aphasia and dense right hemiplegia, suggesting a left hemispheric stroke, and the patient was transferred immediately to a magnetic resonance imaging (MRI) unit. The MR scanner was a whole-body 1.5-T MR system (Signa Horizon, General Electric, Milwaukee, WI) with echo planar imaging (EPI). The scan was performed with a sagittal localizing T1-weighted image (T1WI), followed by axial T1WI, axial DWI, and T2-weighted image (T2WI) with EPI, and intracranial MR angiography. Axial isotropic DWI (single-shot EPI, averaged *x-y-z* directions, b value = 1,000 sec/mm^2, echo/repetition time [TE/TR] = 127/2,000 msec, matrix = 256 × 192, field of view [FOV] = 24 × 24, slice thickness [gap] = 5 [2.5] mm, 14 slices, scan time = 32 seconds) obtained 39 minutes after the ictus onset (11:24 AM) demonstrated an area with diffuse high signals in the left hemisphere (Fig 1). Axial T1WI (fast spoiled gradient-echo, TE/TR = 2.3/60 msec, matrix = 256 × 192, FOV = 20 × 20, thickness [gap] = 5 [2.5] mm, 14 slices, scan time = 1 minute and 34 seconds) and T2WI (EPI, b = 0 sec/mm^2, TE/TR = 127/2,000 msec, matrix = 256 × 192, FOV = 24 × 24, thickness [gap] = 5 [2.5] mm, 14 slices, scan time = 32 seconds) were completely normal. On calculated apparent diffusion coefficient (ADC) maps,[13] the mean ADC ratios (lesion/contralateral sides) were 0.953 ± 0.077 (±SD) in the mesial frontal region of the anterior cerebral artery (ACA) territory, and 0.929 ± 0.080, 0.967 ± 0.061, and 0.989 ± 0.057 in the lateral frontal, superior parietal, and parietotemporal regions of the middle cerebral artery (MCA) territory, respectively. Intracranial three-dimensional time-of-flight MR angiography (fast spoiled gradient-echo, TE/TR = 6.9/37 msec, matrix = 256 × 160, FOV = 14 × 14, slab thickness = 34 mm, 4 slabs, scan time = 13 minutes 49 seconds) obtained 46 minutes after onset showed occlusions in branches of the left ACA and MCA associated with severely decreased signal intensity in the ipsilateral internal carotid artery (ICA) territory (Fig 2). The signal intensity of the left ACA and MCA was slightly higher than the ipsilateral ICA, suggesting an anterograde collateral blood flow through the anterior communicating artery from the contralateral ICA.

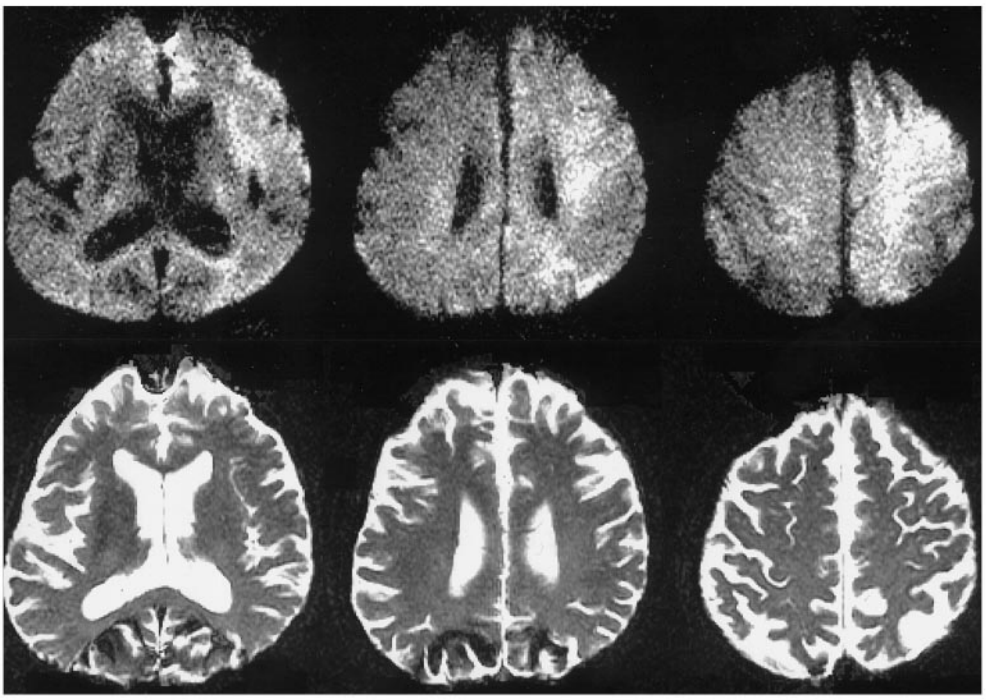

Fig 1. Magnetic resonance imaging (MRI) scans in the hyperacute stage (39 minutes after stroke onset). Axial diffusion-weighted MRI scans (top row) obtained 39 minutes after the ictus onset, demonstrating diffuse high signals in the left hemisphere. Axial T2-weighted (bottom row) and T1-weighted (not shown) images were completely normal.

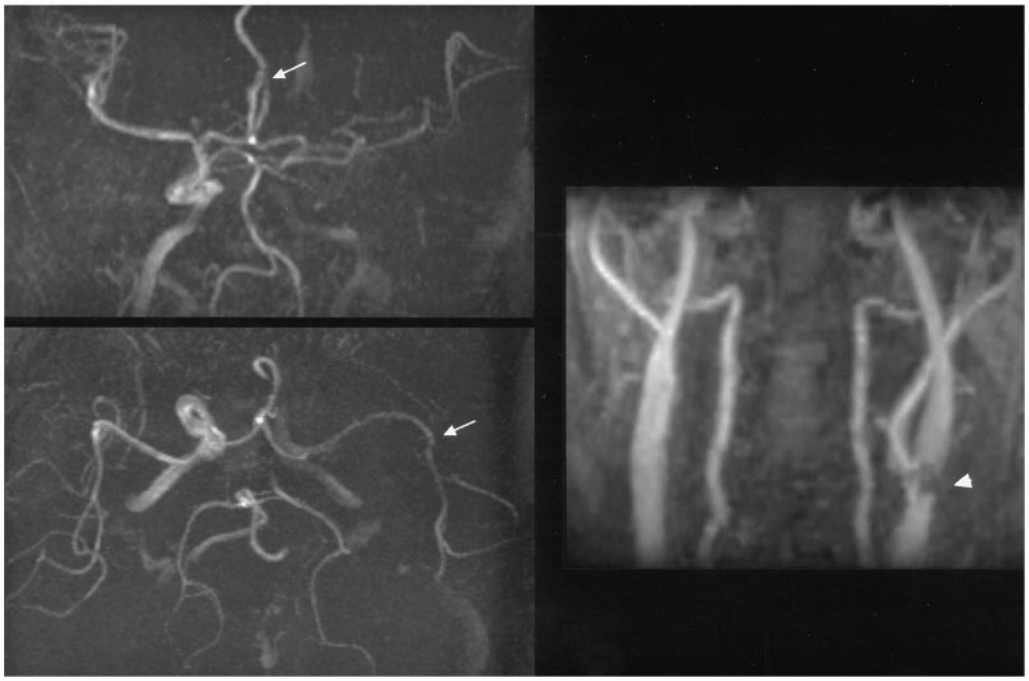

Fig 2. Intracranial magnetic resonance angiographic scans obtained 46 minutes after the ictus (left images) showing occlusions (arrows) *in the left anterior and middle cerebral artery branches, associated with a decreased signal of the ipsilateral internal carotid artery territory. Cervical magnetic resonance angiography (right image) 2 days later showing an atheromatous stenotic lesion* (arrowhead) *in the ipsilateral proximal internal carotid artery.*

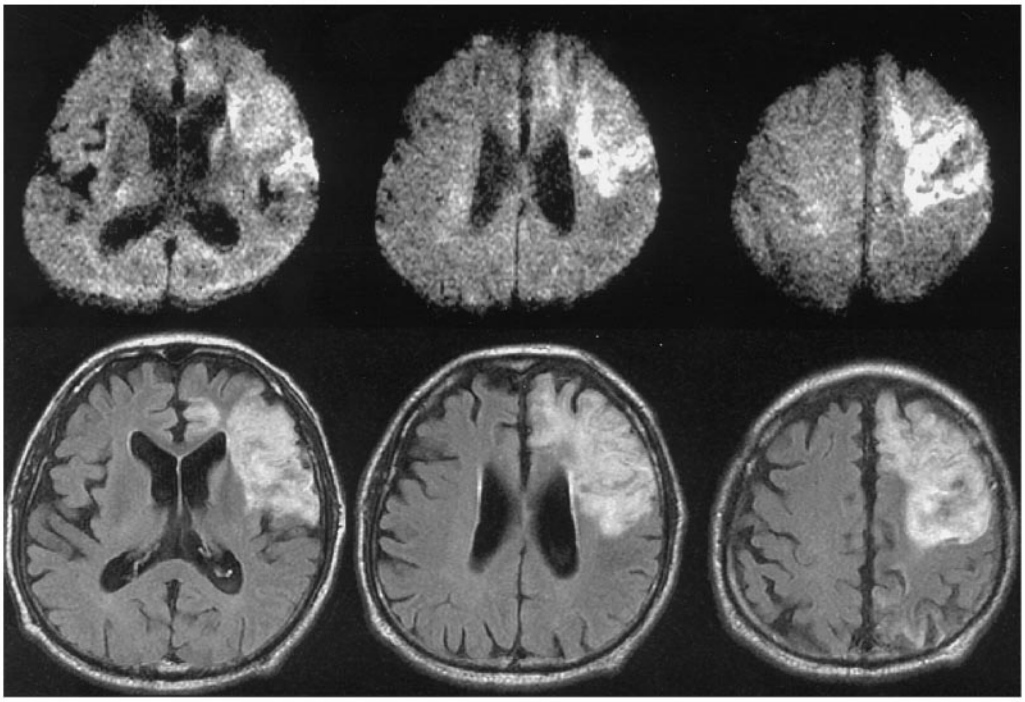

Fig 3. Magnetic resonance imaging (MRI) scans in the chronic stage (23 days after stroke onset). Axial diffusion-weighted MRI scans (top row) showing high signals with partly low-signal spots in the left hemisphere, indicating a hemorrhagic infarction. Axial FLAIR (fluid-attenuated inversion-recovery) images (bottom row) demonstrating an area of high signal with partly low signals. The final infarct size was slightly smaller than the hyperintense area on hyperacute diffusion-weighted images.

A diagnosis of acute cerebral ischemia in the left ICA territory was made, then he was admitted to the stroke care unit of the Hyogo Brain and Heart Center at Himeji, located on the common campus, 75 minutes after the symptom onset (12:00 AM). The National Institutes of Health Stroke Scale score was 21 points. Daily intravenous treatment with 10,000 U of heparin and 500 ml of 10% low molecular dextran solution was started immediately and continued over the next 3 days, followed by 81 mg of aspirin orally daily. A single-photon emission computed tomography (Hitachi 2000H, Tokyo, Japan) with ^{99m}Tc-hexamethylpropyleneamine oxime (HMPAO) 270 minutes after the ictus showed a marked hypoperfusion in the left hemisphere, which was quite similar to the abnormality on the DWI. A brain computed tomography (Toshiba X-force, Tokyo, Japan) 23 hours after the ictus showed a hypodense area in the left ACA and anterior MCA territory. A cervical three-dimensional time-of-flight MR angiography[14] (Siemens Magnetom Impact 1.0 T, Erlangen, Germany) 2 days later demonstrated an atheromatous stenotic lesion in the left proximal ICA (see Fig 2). Repeated axial MRI scans including DWI, T1WI, T2WI, fluid-attenuated inversion-recovery (FLAIR, TE/TR = 147/9,002 msec, matrix = 256 × 192, FOV = 20 × 20, thickness [gap] = 5 [2.5] mm, 14 slices, scan time = 3 minutes 54 seconds) 23 days after stroke onset demonstrated a hemorrhagic infarction in the left ICA territory (Fig 3). The superior part of the left parietal lobe, which had abnormal intensity on the initial DWI and somewhat low ADCs, and the rest of the hemisphere with normal appearance on the initial DWI and normal ADCs, were unaffected by the final infarction on the follow-up MRI scans. A repeated intracranial MR angiography showed a complete reflow in whole branches of the left ICA. The patient was gradually improved to some extent over the next 2 months and discharged with Broca's aphasia and right hemiparesis.

Discussion

In this patient, DWI detected a hyperacute ischemic injury that in the future matured to an infarction 39 minutes after stroke onset. This experience is, to our knowledge, the earliest detection of ischemic insult after onset by DWI in human ischemic stroke. In experimental focal ischemia models, ischemic changes have been demonstrated by DWI as early as 30 minutes after an MCA occlusion.[9–12] We documented this in human stroke. A neurologist witnessed the onset of neurological symptoms in this patient, although in clinical practice a patient's or a witness's report of stroke onset may be unreliable. In addition, a presumed stroke mechanism was an abrupt occlusion of the ACA and MCA branches by artery-to-artery embolic thrombi from an atherosclerotic lesion in the proximal ICA. Therefore, there would be little time lag from actual cerebral arterial occlusion and critical reduction of blood supply to clinical manifestation in this patient. It is unlikely that preonset hemodynamic hypoperfusion because of stenosis in the proximal ICA is involved,

because the stenosis in the left ICA was asymptomatic and moderate in degree.

Previous studies have reported that the final infarct sizes demonstrated by subsequent neuroimagings were larger than or the same as the abnormalities on DWI as early as hours or days after stroke onset.[3,5–7] However, the final infarct size in this patient was slightly smaller than the lesion on the initial DWI, suggesting that the abnormality on earlier DWI includes at least partially reversible ischemic changes after early reperfusion, which can be intervened by treatments as demonstrated in experimental focal ischemia models.[15,16] This report provides important evidence that, as well as in experimental models, DWI detects hyperacute focal cerebral ischemia in minutes after the onset in human stroke, and suggests that DWI is a useful neuroimaging tool in the management of patients receiving thrombolytic, anticoagulant, or neuroprotective therapies.

This study was supported by research grants for cardiovascular disease (9A-2 and 9A-8) from the Ministry of Health and Welfare, Japan.

References

1. Warach S, Chien D, Li W, et al. Fast magnetic resonance diffusion-weighted imaging of acute human stroke. Neurology 1992;42:1717–1723
2. Warach S, Gaa J, Siewert B, et al. Acute human stroke studied by whole brain echo planar diffusion-weighted magnetic resonance imaging. Ann Neurol 1995;37:231–241
3. Sorensen AG, Buonanno FS, Gonzalez RG, et al. Hyperacute stroke: evaluation with combined multisection diffusion-weighted and hemodynamically weighted echo-planar MR imaging. Radiology 1996;199:391–401
4. Lutsep HL, Albers GW, DeCrespigny A, et al. Clinical utility of diffusion-weighted magnetic resonance imaging in the assessment of ischemic stroke. Ann Neurol 1997;41:574–580
5. Baird AE, Benfield A, Schlaug G, et al. Enlargement of human cerebral ischemic lesion volumes measured by diffusion-weighted magnetic resonance. Ann Neurol 1997;41:581–589
6. Lovblad K-O, Baird AE, Schlaug G, et al. Ischemic lesion volumes in acute stroke by diffusion-weighted magnetic resonance imaging correlate with clinical outcome. Ann Neurol 1997;42:164–170
7. Rordorf G, Koroshetz WJ, Copen WA, et al. Regional ischemia and ischemic injury in patients with acute middle cerebral artery stroke as defined by early diffusion-weighted and perfusion-weighted MRI. Stroke 1998;29:939–943
8. Inoue T, Shimizu H, Fujiwara S, et al. Diffusion-weighted MRI detectability of acute cerebral ischemia: comparison with eventual infarction [in Japanese]. No To Shinkei 1998;50:555–560
9. Moseley ME, Kucharczyk J, Mintorovitch J, et al. Diffusion-weighted MR imaging of acute stroke: correlation with T2-weighted and magnetic susceptibility-enhanced MR imaging in cats. AJNR 1990;11:423–429
10. Mintorovitch J, Moseley ME, Chileuitt L, et al. Comparison of diffusion- and T2-weighted MRI for the early detection of cerebral ischemia and reperfusion in rats. Magn Reson Med 1991;18:39–50
11. Minematsu K, Li L, Fisher M, et al. Diffusion-weighted magnetic resonance imaging: rapid and quantitative detection of focal brain ischemia. Neurology 1992;42:235–240
12. Perez-Trepichio AD, Xue M, Ng TC, et al. Sensitivity of magnetic resonance diffusion-weighted imaging and regional relationship between the apparent diffusion coefficient and cerebral blood flow in rat focal cerebral ischemia. Stroke 1995;26:667–674
13. de Crespigny AJ, Marks MP, Enzmann DR, Moseley ME. Navigated diffusion imaging of normal and ischemic human brain. Magn Reson Med 1995;33:720–728
14. Uehara T, Mori E, Ohsumi Y, et al. Usefulness of three-dimensional time-of-flight MR angiography for evaluation of carotid artery bifurcation stenosis. Cerebrovasc Dis 1995;5:199–203
15. Minematsu K, Li L, Sotak CH, et al. Reversible focal ischemic injury demonstrated by diffusion-weighted magnetic resonance imaging in rats. Stroke 1992;23:1304–1310
16. Lo EH, Matsumoto K, Pierce AR, et al. Pharmacologic reversal of acute changes in diffusion-weighted magnetic resonance imaging in focal cerebral ischemia. J Cereb Blood Flow Metab 1994;14:597–603

The Postmigrational Development of Polymicrogyria Documented by Magnetic Resonance Imaging from 31 Weeks' Postconceptional Age

Terrie E. Inder, MD,* Petra S. Huppi, MD,†
Gary P. Zientara, PhD,‡ Ferenc A. Jolesz, MD,‡
Erik E. Holling, BA,† Richard Robertson, MD,§
Patrick D. Barnes, MD,§ and Joseph J. Volpe, MD*

We report the case of a 27-week premature infant in whom magnetic resonance imaging (MRI) at 4 postnatal weeks (postconceptional age, 31 weeks), term, and 6 months of age documented the postnatal postmigrational evolution of bilateral perisylvian polymicrogyria. The polymicrogyria was readily detected by ultrafine 1.5-mm coronal slices on three-dimensional, Fourier-transformed, spoiled gradient–recalled and T2-weighted MRI sequences. These MRI sequences provide the first in vivo documentation of the postmigrational evolution of polymicrogyria. The likelihood that the polymicrogyria was related to an ischemic encephaloclastic mechanism is supported by the simultaneous occurrence of periventricular leukomalacia.

Inder TE, Huppi PS, Zientara GP, Jolesz FA, Holling EE, Robertson R, Barnes PD, Volpe JJ. The postmigrational development of polymicrogyria documented by magnetic resonance imaging from 31 weeks' postconceptional age. Ann Neurol 1999;45:798–801

Polymicrogyria of the cerebral cortex is a developmental abnormality characterized by excessive surface convolution.[1] Two major histological varieties of polymicrogyria are recognized: an unlayered type and a "classic" layered type. The unlayered type is considered to be a disorder of neuronal migration and includes neuronal heterotopias as well as lack of cortical lamination. The layered type includes a four-layered cortex that contains normal neuronal layering, except for the replacement of the deeper cortical layers by an area of laminar necrosis. A role for intrauterine ischemia after termination of cortical neuronal migration in the genesis of the layered variety has been suggested by neuropathological studies.[2,3] Our case describes the postmigrational development of polymicrogyria detected by ultrafine slices on serial magnetic resonance imaging (MRI) sequences for the first time in the living infant.

Case Report

The male infant was born to a 33-year-old gravida 1 para 0 mother following an unremarkable twin pregnancy. At 27 weeks' gestation, she presented in preterm labor. There was no evidence of fetal distress, and no maternal fever was documented. Delivery was by Cesarean section 1 hour after rupture of membranes due to breech presentation of the first twin. At delivery, the case infant, the second twin, was intubated in the delivery room for respiratory distress. Apgar scores were 6 at 1 minute and 7 at 5 minutes. His admission weight was 1,165 g (50th percentile for gestational age), and his head circumference was 29 cm (80th percentile for gestational age). His initial hospital course included ventilator dependency for a period of 17 days. He received dopamine and hydrocortisone therapy for the first 3 postnatal days for hypotension. The first cranial ultrasound scan at 1 day of age showed small bilateral intraventricular hemorrhages. A repeat cranial ultrasound at 3 days of age demonstrated additional abnormalities (ie, prominent periventricular echodensities in the left frontoparietal and bilateral parieto-occipital regions). This abnormal parenchymal echogenicity evolved over 3 weeks to multiple echolucent periventricular lesions consistent with cystic periventricular leukomalacia (Fig, A). At 4 weeks of age (31 weeks' postconceptional age), the infant was scanned in a 1.5-T General Electric Signa MRI system (Milwaukee, WI). For the acquisition of primary MRI data, two different imaging modes were applied: a three-dimensional, Fourier-transformed, spoiled gradient–recalled sequence with 1.5-mm slices as well as a double-echo proton density and T2-weighted spin-echo sequence with 3-mm slices.[4] The MRI sequence at 4 postnatal weeks showed a minor abnormality in the perisylvian region of uncertain significance as well as findings consistent with the small intraventricular hemorrhages and marked bilateral periventricular leukomalacia (see Fig, B). MRI with diffusion-weighted images showed an elevation in the apparent diffusion coefficient in the periventricular cerebral white matter at the sites of the apparent cystic lesions, a finding suggesting that the periventricular lesions were chronic. Subsequent MRI sequences at 13 weeks of age (term equivalent) (see Fig, C and D) and at 6 months of age (corrected age of 3 months) showed marked evolution of extensive bilateral perisylvian cortical polymicrogyria as well as the presence of bilateral periventricular cystic changes with mineralization.

From the *Department of Neurology, Children's Hospital and Harvard Medical School, †Joint Program in Neonatology, Harvard Medical School and Department of Pediatrics, University of Geneva, Geneva, Switzerland, ‡Department of Radiology and Magnetic Resonance Imaging Division, Brigham and Women's Hospital and Harvard Medical School, and §Division of Neuroradiology, Department of Radiology, Children's Hospital and Harvard Medical School, Boston, MA.

Received Nov 30, 1998, and in revised form Feb 17, 1999. Accepted for publication Feb 18, 1999.

Address correspondence to Dr Volpe, Neurology Department, Fegan 1103, Children's Hospital, 300 Longwood Avenue, Boston, MA 02115.

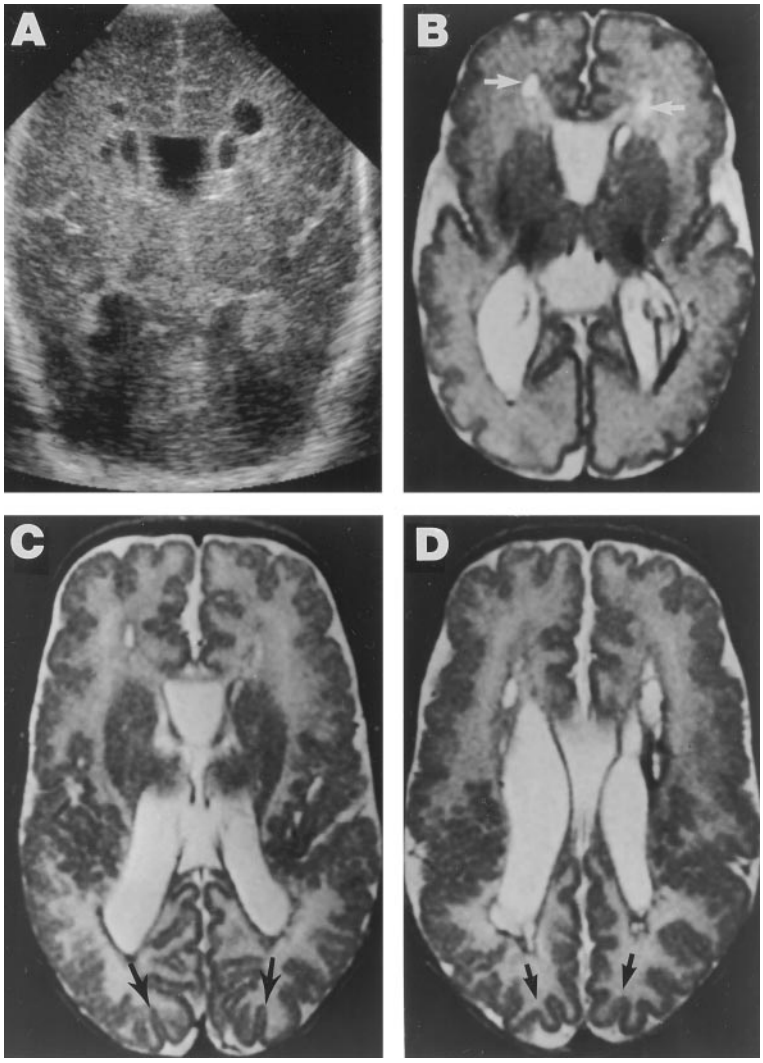

Fig. (A) Coronal ultrasound scan at 3 weeks of age. There are multiple echolucent lesions in the periventricular regions. (B) Axial T2-weighted magnetic resonance imaging (MRI) scan taken at 4 weeks of age (31 weeks' postconceptional age) demonstrating findings consistent with small intraventricular hemorrhage and cystic periventricular leukomalacia (white arrows). *The perisylvian region is not clearly abnormal. (C and D) Axial T2-weighted MRI scans taken at 13 weeks of age (ie, term equivalent), demonstrating marked evolution of perisylvian cortical microgyria with relative sparing of the occipital cortex* (black arrows) *as well as bilateral periventricular cystic changes with mineralization.*

Discussion

This case report is important because it describes for the first time the postmigrational development of an apparent encephaloclastic polymicrogyria. The association with the evolution of cystic periventricular leukomalacia and the findings on diffusion-weighted imaging support the conclusion that ischemia was an important pathogenic mechanism. Moreover, the findings have implications for the pathogenesis of "congenital bilateral perisylvian polymicrogyria."

Two anatomical forms of polymicrogyria, "classic" layered and unlayered, can be distinguished by microscopic appearance.[1] The layered type is characterized by four layers: a relatively intact outermost molecular layer, a similarly preserved and richly cellular upper cortical layer, a cell-poor gliotic layer of apparent laminar cortical necrosis, and a relatively preserved deep layer of intact neurons. A principal cause of this form of polymicrogyria appears to be ischemia, with the occurrence of laminar cortical necrosis. Indeed, this type of polymicrogyria often coexists at the margins of more severe ischemic or destructive lesions (eg, hydranencephaly) or in association with destructive infectious processes.[3] Williams and Caviness[5] concluded from the detailed analysis of their case that the deep cell-sparse layer of the four-layered type represented neuronal loss and glial replacement similar to that of laminar cortical necrosis in the adult with hypoxic-ischemic injury. Their conclusion was supported by Golgi analysis of neuronal subtypes in the layers of the microgyric cortex, which indicated that the neuronal classes present were in their proper positions.[5] Another recognized cause of layered polymicrogyria is intrauterine infection, particularly cytomegalovirus. In this disorder, indirect evidence suggests that polymicrogyria is not caused by direct viral attack but results from general perfusion failure.[6] Our patient had no evidence of cytomegalovirus infection by serum titers and urine culture.

In the nonlayered variety of polymicrogyria, the neurons destined primarily for the outer cortical layers ap-

pear to have been impeded in their migrations. This disturbance results in a cortical surface with multiple plications and a poorly or nonlaminated cortex with heterotopic neurons in cerebral white matter. This disorder of neuronal migration appears to occur no later than the fourth to fifth month of gestation, that is, in the final phase of neuronal migration for cortical development. That this variety of polymicrogyria can be related to an abnormality of the developmental program for neuronal migration is supported by its occurrence in the cerebro-hepato-renal syndrome of Zellweger.[7] In the nonlayered form of polymicrogyria, ischemia during neuronal migration may also be a pathogenic mechanism. Thus, this lesion has been documented in early feto-feto transfusion syndromes in both donor[8,9] and recipient twins.[10] These cases involved monochorionic twins, with the death of 1 twin at 13 to 16 weeks of gestation. Our patient is a dichorionic twin with an uncomplicated pregnancy, a surviving unaffected twin, and evolution after 31 weeks of gestation.

Polymicrogyria has a variable appearance on MRI studies depending on the technique(s) used. On routine, 5-mm, spin-echo sections, polymicrogyria has the appearance of thickened cortex with irregularity of the gray-white junction.[11,12] Higher resolution of the cortex can be obtained by using thinner sections, smaller fields of view, and more phase-encoding steps. We used a three-dimensional, Fourier-transformed, spoiled gradient–recalled sequence with 1.5-mm coronal slices and a T2-weighted sequence with 3-mm axial slices. These sequences were quite sensitive for the early detection of the cortical abnormality in this infant, and this communication reports the earliest described MRI detection of polymicrogyria.

The histopathology of the polymicrogyria in our patient is not known. The absence of evidence of heterotopias on ultrafine-slice MRI is consistent with a layered polymicrogyria. Our hypothesis is that this infant suffered a major ischemic insult in the perinatal period, probably shortly after birth. This insult resulted in ischemia both to the periventricular white matter, with the subsequent ultrasonographic evolution from periventricular echodensities to echolucencies that is consistent with the development of cystic periventricular leukomalacia, and to the cortical neurons, with the subsequent development of cortical neuronal necrosis. The latter occurrence led to the development of the bilateral polymicrogyria of the layered type. This timing is supported by the evolution of the radiological findings. An alternative hypothesis for the development of polymicrogyria in our patient is that the marked cerebral white matter injury played a causal role. Thus, theoretical modeling and experimental observations suggest that the fiber development in cerebral white matter is crucial to gyral development. With major white matter injury as in our case, such "tension-based morphogenesis" might be impaired.[13] There are no prior reports of the coexistence of cystic periventricular leukomalacia and polymicrogyria. This lack could be due to difficulties with conventional MRI, computed tomography, and ultrasonography in detection of the cortical lesion.

Congenital bilateral perisylvian polymicrogyria has become recognized as a form of focal polymicrogyria.[14] This developmental disorder usually presents in infancy and childhood with the clinical features of facial diplegia, dysarthria, pseudobulbar palsy, mild to severe mental retardation, and seizures. The condition was originally recognized due to its similarity to the acquired syndrome of fasciopharyngoglossomasticatory diplegia resulting from bilateral infarction of the anterior operculum as described by Foix and co-workers[15] in 1926. Relatively few pediatric cases of congenital bilateral perisylvian syndrome have been reported. Subsequent to the original description by Grad-Radford and colleagues[16] in 1986, 30 childhood cases have been reported.[14,17] Gropman and co-workers[12] described the largest series (12 cases) presenting in childhood and identified by MRI. There has been no previously reported association with premature birth or periventricular leukomalacia.

This work was supported by grants from the Swiss National Foundation, Sigrist Foundation of the University of Berne, and the Charles A. Janeway Scholarship Fund in Child Health Research to Dr Huppi and a grant from the National Institutes of Health (HD-18655) to Dr Volpe.

References

1. Volpe JJ. Neurology of the newborn. 3rd ed. Philadelphia: WB Saunders, 1995
2. De Leon GA. Observations on cerebral and cerebellar microgyria. Acta Neuropathol (Berl) 1972;20:278–287
3. Richman DP, Stewart RM, Caviness VS, Jr. Cerebral microgyria in a 27-week fetus: an architectonic and topographic analysis. J Neuropathol Exp Neurol 1974;33:374–378
4. Huppi PS, Warfield S, Kikinis R, et al. Quantitative magnetic resonance imaging of brain development in premature and mature newborns. Ann Neurol 1998;43:224–235
5. Williams RS, Caviness VS, Jr. The cellular pathology of microgyria: a Golgi analysis. Acta Neuropathol (Berl) 1976;36: 269–283
6. Dias MJM, Harmant-van Rijckevorsel G, Landneu P, et al. Prenatal cytomegalovirus disease and cerebral microgyria: evidence for perfusion failure, not disturbance of histogenesis, as the major cause of fetal cytomegalovirus encephalopathy. Neuropediatrics 1984;15:18–24
7. Volpe JJ, Adams RD. Cerebro-hepato-renal syndrome of Zellweger: an inherited disorder of neuronal migration. Acta Neuropathol (Berl) 1972;20:175–198
8. Barth PG, van der Harten JJ. Parabiotic twin syndrome with topical isocortical disruption and gastroschisis. Acta Neuropathol (Berl) 1985;67:345–349
9. Norman MG. Bilateral encephaloclastic lesions in a 26-week gestation fetus: effect on neuroblast migration. Can J Neurol Sci 1980;7:191–194

10. Sugama S, Kusano K. Monozygous twin with polymicrogyria and normal co-twin. Pediatr Neurol 1994;11:62–63
11. Barkovich AJ, Kuzniecky RI. Neuroimaging of focal malformations of cortical development. J Clin Neurophysiol 1996;13: 481–494
12. Gropman AL, Barkovich AJ, Vezina LG, et al. Pediatric congenital bilateral perisylvian syndrome: clinical and MRI features in 12 patients. Neuropediatrics 1997;28:198–203
13. Van Essen DC. A tension-based theory of morphogenesis and compact wiring in the central nervous system. Nature 1997; 385:313–318
14. Guerrini R, Dravet C, Raybaud C, et al. Neurological findings and seizure outcome in children with bilateral opercular macrogyric-like changes detected by MRI. Dev Med Child Neurol 1992;34:694–705
15. Foix C, Chavany JA, Marie J. Diplegie facio linguomasticatrice d'origin cortico-sous-corticale sans paralysie des membres. Rev Neurol (Paris) 1926;33:214–219
16. Graff-Radford NR, Bosch EP, Stears JC, Tranel D. Developmental Foix-Chavany-Marie syndrome in identical twins. Ann Neurol 1986;20:632–635
17. Kuzniecky R, Andermann F, Tampier D, et al. Bilateral central macrogyria: epilepsy, pseudobulbar palsy, and mental retardation: a recognizable neuronal migration disorder. Ann Neurol 1989;25:547–554

Extensive Cerebral White Matter Abnormality without Clinical Symptoms: A New Hereditary Condition?

T. Autti, MD,* M. Muttilainen, MD,†
R. Raininko, MD,‡ H. Heiskala, MD,§ J. Puranen, BM,‖
A.-M. Häkkinen, PhD,*‖ P. Tienari, MD,††
P. Santavuori, MD,# P. Suominen, MD,¶
and M. Somer, MD**

A 30-year-old father and his 2 sons with slight hyperkinesia and mildly dysmorphic features and their close relatives were examined clinically and with computed tomography (CT) and magnetic resonance imaging (MRI). Neurophysiological and biochemical examinations were normal; however, brain MRI of the father and sons revealed extensive cerebral white matter changes. No radiological progression could be detected at a 13-year follow-up examination of the father, and proton magnetic resonance spectroscopy (MRS) of the father at the age of 30 years was normal. MRI findings in the relatives were normal, suggesting an autosomal dominant syndrome due to a new mutation in the father.

From the Departments of *Radiology, ††Neurology, ‖Oncology, and ‖Anaesthesiology, Helsinki University, #Department of Paediatric Neurology, Hospital for Sick Children and Adolescents, Helsinki University, and **Department of Medical Genetics, The Family Federation of Finland, Helsinki, and †Department of Paediatrics, Jorvi Hospital, and §Rinnekoti Foundation, Espoo, Finland; and ‡Department of Diagnostic Radiology, Uppsala University, Uppsala, Sweden.

Received Dec 14, 1998, and in revised form Feb 14, 1999. Accepted for publication Feb 19, 1999.

Address correspondence to Dr Autti, Department of Radiology, Central Hospital University of Helsinki, Haartmaninkatu 4, FIN-00290 Helsinki, Finland.

Autti T, Muttilainen M, Raininko R, Heiskala H, Puranen J, Häkkinen A-M, Tienari P, Santavuori P, Suominen P, Somer M. Extensive cerebral white matter abnormality without clinical symptoms: a new hereditary condition? Ann Neurol 1999;45:801–805

The leukodystrophies are disorders characterized by primary involvement of the white matter caused by enzyme deficiencies. Most leukodystrophies are inherited as autosomal or X-linked recessive traits, and autosomal dominant leukodystrophies are rare.[1–12] In the infantile and juvenile forms, the patients have progressive mental retardation and premature death. In the adult form, the symptoms are usually milder, and progression of the disease is slower.

Leukodystrophy-like brain alterations have been reported in patients in whom the course of the disease is nonprogressive. This group may include nonleukodystrophic white matter diseases of many different etiologies.[13] In 18q-syndrome, for example, dysmyelination is the most prominent finding. These patients usually have mental retardation in addition to facial dysmorphism, syndactyly, and behavioral problems.[14]

We report a new, clinically benign, probably autosomal dominant, nonprogressive condition with extensive white matter abnormalities detected by means of magnetic resonance imaging (MRI) in midchildhood.

Case Histories

Subject 1

The early development of this 30-year-old man was normal. At the age of 3 years, the short soft palate was noticed because of his nasal voice. The mandibular rami were hypoplastic. An audiogram was normal. At the age of 4 years, he was in a car accident, at which time, he experienced brief unconsciousness. After the accident, he was recorded as having a symmetrical midfrequency sensorineural hearing loss, necessitating a hearing aid. During his early school years, hyperkinesia was recorded.

At the age of 18 years, he was re-examined because of recurrent headaches. Computed tomography (CT) showed hypodense cerebral white matter, located mostly in the frontal lobes, but some changes could also be seen in the parietal and occipital lobes. No neurological abnormalities were noticed; however, he had mildly dysmorphic facial features with hypertelorism, bushy eyebrows, synophrys, asymmetrical pal-

pebral fissures, and asymmetrical auricles. He had hyperopia (+6 diopters), mild exophoria, and tortuous retinal veins. One year later, CT showed no progression. Peripheral blood chromosome analysis with G-banding showed a normal karyotype.

CT findings were unchanged in this patient at the age of 29 years, when similar CT alterations were found in his sons. Muscle strength was normal, but tendon reflexes were weak. There was no progression of the hearing loss. Neuropsychological tests showed his memory and reasoning ability to be better than average.

At the ages of 29 and 30 years, this patient underwent MRI with T2- and proton density–weighted spin-echo sequences, and a FLAIR sequence showed large frontoparietal changes of high signal intensity. The changes showed low signal intensity on T1-weighted images (Fig 1A and B). The arcuate fibers were preserved. The frontal and parietal pathological areas were partially separated, with the pre- and postcentral gyri being almost intact; small isolated hyperintensities were detected in the posterior temporal white matter. No pathological changes were seen in the insular areas. The corpus callosum and internal capsules were normal. Some changes were seen in the vicinity of the occipital horns, mostly lateral to and above the proximal parts. The optic radiations were spared. The cerebellum and brainstem were normal. No atrophy was found. Proton magnetic resonance spectroscopy (MRS) (STEAM sequence: TE = 20 and 270 msec, TR = 300 msec) at the age of 30 years was normal.

Subject 2

The boy was delivered by emergency Cesarean section after a 30-week gestation because of acute placental bleeding. His birth weight was 1400 g, and he had Apgar scores of 8. His psychomotor development was normal. His first skull ultrasound examination at the age of 1 month showed slight asymmetrical ventricular dilatation.

At the age of 6 years, he was sent for neurological evaluation because of hyperkinesia and slight motor clumsiness. He had scaphocephaly with a normal-sized skull, a high frontal hairline, a triangular face, upslanting palpepral fissures, a short nose, abnormal auricles, and a small chin. There was mild cutaneous syndactyly of his second and third fingers as well as his third and fourth fingers. The audiogram was normal. He had strabismus convergens. At the age of 7 years, his Wechsler Scale of Intelligence (WISC-R) verbal IQ was 108 and his performance IQ was 96, for a total IQ of 102. A neuropsychological examination identified problems in impulse control and visual memory, but he had good verbal skills and learning capacity.

He had problems in concentration and started school 1 year later than usual. After 2 years of occupational therapy, he was doing well in a normal school. CT and MRI at the

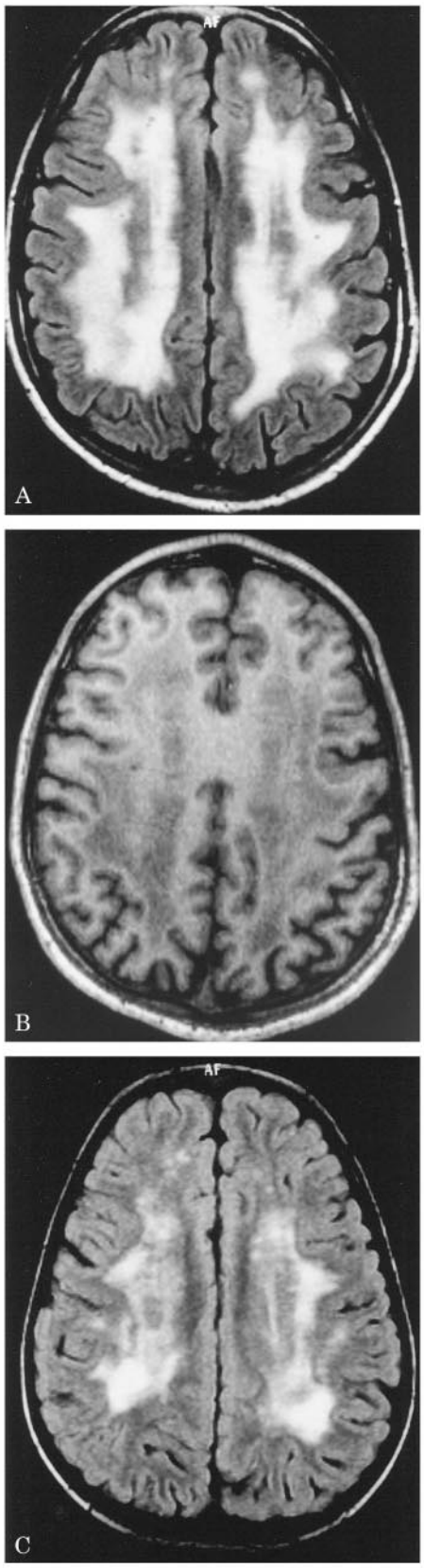

Fig 1. Magnetic resonance imaging (MRI) (FLAIR sequence) of the healthy 30-year-old man shows a large area of (A) high signal intensity and (B) low signal intensity on a T1-weighted image in the frontal and parietal white matter. The subcortical white matter is not affected. (C) MRI (FLAIR sequence) of the 6-year-old boy shows a large area of high signal intensity in the frontal and parietal white matter.

ages of 7 and 9 years, respectively, showed changes similar to those seen in his father.

Subject 3

The second boy was delivered by emergency Cesarean section because of threatening asphyxia after 31 weeks of gestation. His birth weight was 1370 g, and he had Apgar scores of 10. Skull ultrasound examinations were normal. He showed delayed speech evolution at the age of 18 months and had speech therapy for 2 years, reaching normal language milestones at the age of 6 years.

At the age of 4 years, brain CT showed changes similar to those seen in his brother and father (see Fig 1C). He had a large head (+1.5 SD) for his height (−0.5 SD) and similar mildly dysmorphic features as his brother. He had strabismus convergens. The ocular fundi were normal. The audiogram was normal.

In a neuropsychological examination at the age of 5 years, his WISC-R verbal IQ was 98 and his performance IQ was 68, for a total IQ of 78. His visuomotor age was 3 years and 11 months, and his standard score was 84. He was a talkative and playful child, having significant problems in impulse control.

MRI at the age of 6 years showed changes similar to those seen in his father and brother. The frontal and parietal pathological areas were not so well separated as in Subjects 1 and 2, but no changes were found in the pre- or postcentral gyri.

Biochemical and Neurophysiological Examinations

All subjects had normal biochemical examinations, including urinary amino acid screening; arylsulfatase and sulfatide levels; and quantitative assays of plasma amino acids, serum cortisol, and very long chain fatty acids. Electroencephalographic, visual evoked potential, and motor and sensory conduction velocity examinations were also normal.

Chromosome 18 Analysis

The terminal deletions of the 18q chromosome may delete one copy of the myelin basic protein (MBP) gene. We

Fig 2. The pedigree shows the proband (arrow) *and his sons with magnetic resonance imaging (MRI) findings resembling those of leukodystrophy* (half-shaded symbols). *The family members with normal brain MRI findings are marked with (N). There is also sensorineural hearing loss in several family members* (symbols with shaded upper quadrant) *with apparent autosomal dominant inheritance. Segregation of chromosome 18q haplotypes (myelin basic protein, D18S462, D18S871) demonstrate that there is no evidence of a deletion characteristic of 18q syndrome. These markers cover approximately 1 Mb of DNA; the estimated distance to 18qter is 2.5 Mb.*

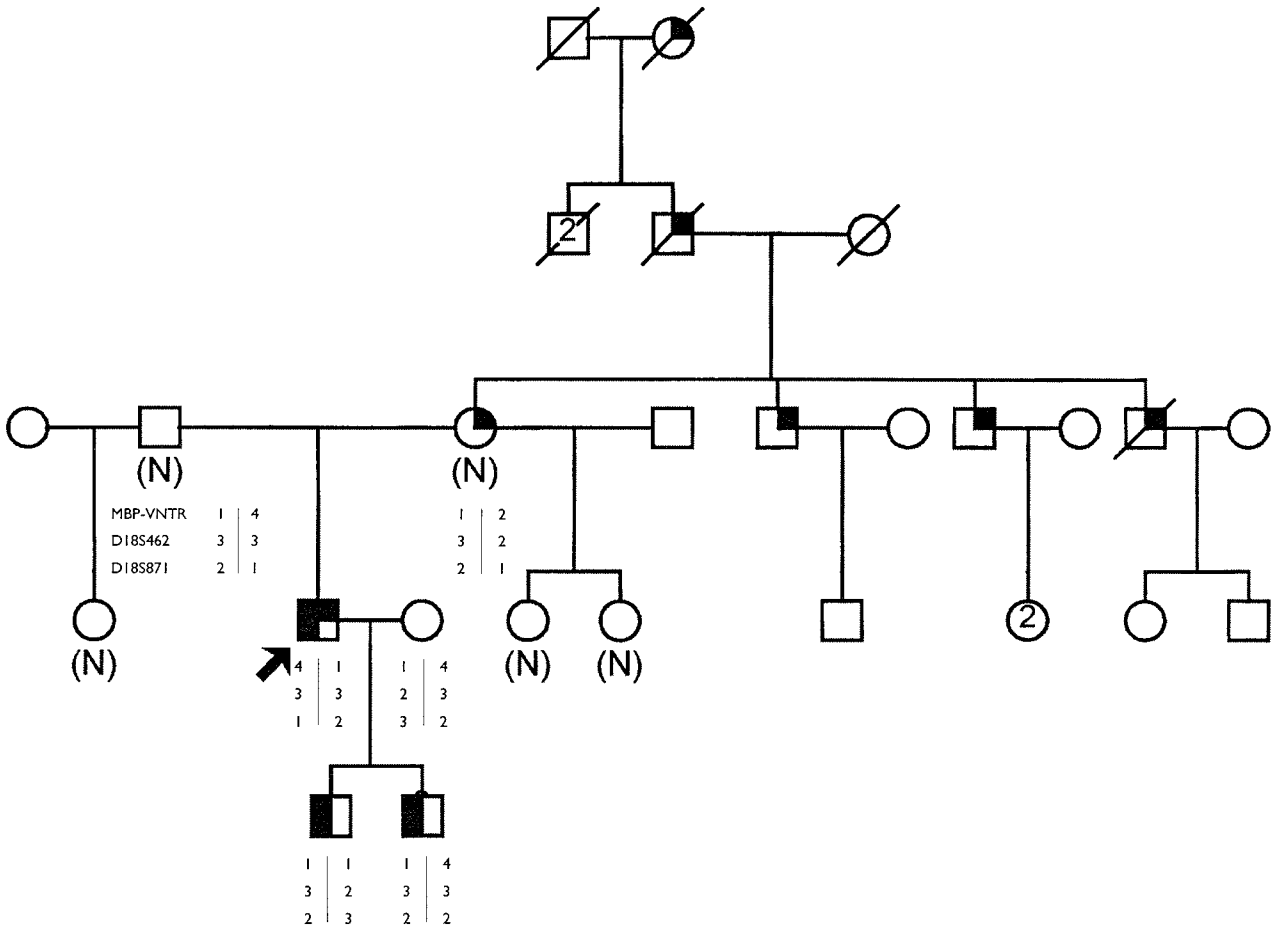

analyzed the segregation of three markers on chromosome 18q22–q23, namely, MBP-VNTR, D18S462, and D18S871, which together encompass approximately 1 Mb of DNA. As shown in Figure 2, there was no evidence for a deletion (hemizygocity) of this genomic region.

Relatives

The father and 3 half-sisters of Patient 1 had no neurological symptoms. The mother had mild sensorineural hearing loss, which she presumably inherited from her father. All relatives had normal MRI findings; however, there were several other relatives with hearing defects (see Fig 2).

Discussion

We describe a subjectively healthy 30-year-old father and 2 sons, all of whom had striking white matter alterations on brain MRI. To the best of our knowledge, no discrepancy of this kind between clinical condition and brain imaging findings resembling leukodystrophy has been previously reported. An absence of similar findings in close relatives of the father suggests that this is a previously unknown autosomal dominant condition (due to a new mutation in the father).

These neuroimaging abnormalities of our subjects may be speculated to represent a preclinical manifestation of an autosomal dominant leukodystrophy with adult onset. Such leukodystrophies have been found with clinical features resembling those of multiple sclerosis, but usually not occurring before the fourth to fifth decade of life.[1,2,4,6–9,11,12] Imaging studies of adult onset leukodystrophies[8,9,11] have included a total of 18 symptomatic subjects and 18 asymptomatic relatives. In the symptomatic patients, the alterations on MRI resembled those seen in our subjects; in addition, cerebellar and brainstem abnormalities were frequently seen. In 16 asymptomatic relatives aged 18 to 63 years, MRI findings were normal. Two asymptomatic men, 30 and 36 years of age, had focal alterations in the frontoparietal cerebral white matter; in addition, the younger subject had cerebellar alterations. The areas of the cerebral abnormalities were much smaller than in our subjects. The older patient had an abnormal somatosensory evoked potential as did all of the patients with clinical symptoms and abnormal MRI findings.[11,12]

MRI studies of multiple sclerosis patients[15] and an animal model of multiple sclerosis[16] have demonstrated that severe demyelination can occur in neurologically normal subjects. The nonprogressive nature of the white matter abnormalities and of the clinical symptoms in this family indicates that this syndrome is probably not a demyelinating disorder.[13] This is supported by the normal proton MRS, indicating that MRI alterations are not due to demyelination[17,18] as has been found in autopsied cases of adult onset leukodystrophies.[1,2,5,8]

The disorder in our family may be due to a mutation in an autosomal dominant gene such as the MBP gene, leading to abnormal structure of the myelin. Failure of MBP gene expression[19] and polymorphism at the MBP locus[20] are correlated with extrapyramidal and other neurological symptoms, however. In our subjects, there was no evidence of MBP deletion.

It remains unclear as to whether the sensorineural hearing loss in the father of this family is in any way related to the white matter abnormality of the brain. He may have inherited it from his nonaffected mother as an autosomal dominant trait. It is worth noting that some patients with adult onset leukodystrophy have sensorineural deafness.[8]

In conclusion, the severely affected cerebral white matter and sparing of the white matter beneath the sensorimotor cortex and the optic radiation, the normal proton MRS, the negative laboratory tests, neurophysiological examinations, and the mild dysmorphic features in our family suggest a previously undescribed condition with probable autosomal dominant inheritance. The parents and 3 half-sisters of the father had normal brain imaging findings, suggesting a new mutation in the father.

This work was supported by grants from the Ulla Hjelt Memorial Fund awarded by the Foundation for Paediatric Research.

References

1. Camp CD, Löwenberg K. An American family with Pelizaeus-Merzbacher disease. Arch Neurol Psychiatry 1941;45:261–264
2. Zerbin-Rüdin E, Peiffer J. Ein genctischer heitrag zur frage der spätform der Pelizaeus-Merzbacherchen Krankheit. Humangenetik 1964;1:107–122
3. Oepen H. Klinische, pathologisch-anatomische und genealogische Unterschung einer spätadulten Leukodystrophie. Arch Psychiatr Z Ges Neurol 1964;206:115–130
4. Peiffer J, Zerbin-Rüdin E. Zur Variationsbreite der Pelizaeus-Merzbacherchen Krankheit (Zugleich ein Beitrag zur familiären Multiplen Sklerose). Acta Neuropathol (Berl) 1963;3:87–107
5. Löwenberg K, Hill TS. Diffuse sclerosis with preserved myelin island. Arch Neurol Psychiatry 1933;29:1232–1245
6. Eldridge R, Anatoys CP, Schlesinger S, et al. Hereditary adult-onset leukodystrophy simulating chronic progressive multiple sclerosis. N Engl J Med 1984;311:948–953
7. Schwankhaus JD, Patronas N, Dorwart R, et al. Computed tomography and magnetic resonance imaging in a newly described adult-onset leukodystrophy. Arch Neurol 1988;45: 1004–1008
8. Schwankhaus JD, Katz DA, Eldridge R, et al. Clinical and pathological features of an autosomal dominant, adult-onset leukodystrophy simulating multiple sclerosis. Arch Neurol 1994;51:757–766
9. Abe K, Ibeda M, Watase K, et al. A kindred of hereditary adult-onset leukodystrophy with dominant inheritance and normal arylsulfatase A levels. Neuroradiology 1993;35:281–283
10. Wright GD, Patel MK, Mikel J. An adult onset metachromatic leukodystrophy with dominant inheritance and normal arylsulfatase A levels. J Neurol Sci 1988;87:153–166.
11. Bergui M, Bradac GB, Leombruni S, et al. MRI and CT in an autosomal dominant adult-onset leukodystrophy. Neuroradiology 1997;29:423–426
12. Qattrocolo G, Leombruni S, Vaula G, et al. Autosomal domi-

nant late-onset leukoencephalopathy. Clinical report of a new Italian family. Eur Neurol 1997;37:53–61
13. van der Knaap MS, Valk J. Non-leukodystrophic white matter changes in inherited disorders. Int J Neuroradiol 1995;1:56–66
14. Loevner L, Shapiro R, Grossman R, et al. White matter changes associated with deletions of the long arm of chromosome 18 (18q-syndrome): a dysmyelination disorder? AJNR Am J Neuroradiol 1996;17:1843–1848
15. Filippi M, Paty DW, Kappos L, et al. Correlations between changes in disability and T2-weighted brain MRI activity in multiple sclerosis: a follow-up study. Neurology 1995;45:255–260
16. Rivera-Quinones C, McGavern D, Schmelzer J, et al. Absence of neurological deficits following extensive demyelination in a class I–deficient murine model of multiple sclerosis. Nat Med 1988;4:187–193
17. Kruse B, Hanefeld F, Christen H-J, et al. Alterations of brain metabolites in metachromatic leukodystrophy as detected by localized proton magnetic resonance spectroscopy in vivo. J Neurol 1993;241:68–74
18. Bruhn H, Frahm J, Merboldt K, et al. Multiple sclerosis in children. Cerebral metabolic alterations monitored by localized proton magnetic resonance spectroscopy in vivo. Ann Neurol 1992;34:140–151
19. Iester A, Vignola S, Callegarini L, et al. 18q Syndrome with deficiency of myelin basic protein (MBP). Pediatr Med Chir 1996;18:201–245
20. Tienari PJ, Kuokkanen S, Pastinen T, et al. Golli-MBP gene in multiple sclerosis susceptibility. J Neuroimmunol 1998;81:158–167

Association of Anti-Yo (Type I) Antibody with Paraneoplastic Cerebellar Degeneration in the Setting of Transitional Cell Carcinoma of the Bladder: Detection of Yo Antigen in Tumor Tissue and Fall in Antibody Titers following Tumor Removal

John E. Greenlee, MD,* Josep Dalmau, MD,†
Trek Lyons, BS,* Susan Clawson, BA,*
Richard H. Smith, MD,‡ and H. R. Pirch, MD§

Anti-Yo (type I) autoantibodies reactive with Purkinje cell cytoplasmic antigens of 34 and 62 kd are found in the serum and cerebrospinal fluid of patients with paraneoplastic cerebellar degeneration associated with cancer of the ovary, uterus, adnexa, or breast. Anti-Yo antibody response is rarely associated with other tumors. Here, we present a patient who developed paraneoplastic cerebellar degeneration and anti-Yo antibody response in association with transitional cell carcinoma of the bladder. The presence of anti-Yo antibodies was confirmed by immunofluorescence assay and by Western blot analysis against both Purkinje cell lysates and the CDR62 fusion protein. Yo antigen was demonstrated in sections of the patient's tumor. Antibody titers fell after tumor removal. Transitional cell carcinoma should be considered in patients presenting with subacute cerebellar degeneration and anti-Yo antibody response in whom ovarian, adnexal, uterine, or breast cancer cannot be detected.

Greenlee JE, Dalmau J, Lyons T, Clawson S, Smith RH, Pirch HR. Association of anti-Yo (type 1) antibody with paraneoplastic cerebellar degeneration in the setting of transitional cell carcinoma of the bladder: detection of Yo antigen in tumor tissue and fall in antibody titers following tumor removal. Ann Neurol 1999;45:805–809

From the *Neurology Service, Veterans Affairs Medical Center and Department of Neurology, University of Utah School of Medicine, Salt Lake City, UT; †Department of Neurology, Memorial Sloan-Kettering Cancer Center, New York, NY; ‡Neurospecialty Associates and §Saint Anthony's Hospital, Denver, CO.

Received Jul 23, 1998, and in revised form Feb 18, 1999. Accepted for publication Feb 19, 1999.

Address correspondence to Dr Greenlee, Neurology Service (127), Veterans Affairs Medical Center, 500 Foothill Drive, Salt Lake City, UT 84148.

Type I ("anti-Yo") antibodies are autoantibodies found in the serum and cerebrospinal fluid of patients with paraneoplastic cerebellar degeneration.[1–3] These antibodies recognize cytoplasmic antigens of Purkinje cells and label proteins of 34 and 62 kd in blots of Purkinje cell lysates.[1–5] Anti-Yo antibodies are almost invariably associated with adenocarcinomas of the ovary, uterus, adnexa, and breast, and the presence of anti-Yo antibody response has been used as a marker for these tumors in adults presenting with subacute cerebellar degeneration.[6,7] Anti-Yo antibody response is rarely associated with other tumor types.[1,3,6–8] Here, we describe a 64-year-old woman with paraneoplastic cerebellar degeneration in whom anti-Yo antibody response was associated with transitional cell carcinoma of the bladder.

Patient Summary

A 64-year-old woman was in good health until March 10, 1991, when she awoke with nausea, vomiting, vertigo, headache, and intermittent double vision. Her symptoms persisted, and she presented for evaluation on March 29, 1991. Her past health was unremarkable, except for a hysterectomy many years before.

The results of her general physical examination were unremarkable. A neurological examination revealed coarse nystagmus on right lateral gaze. The cranial nerves were otherwise intact. The results of motor and sensory examinations were normal. Her station was normal, and Romberg's sign was absent. Her gait was broad-based, however, and she had difficulty with tandem gait. Her reflexes were symmetrical throughout, and Babinski's sign was absent. The hematological studies were normal, except for an erythrocyte sedimentation rate of 45 mm/hr. Magnetic resonance imaging (MRI) showed a small area of increased signal in the white matter of the right frontal lobe, which was consistent with old ischemic injury. The patient was thought to have a viral labyrinthitis.

The patient remained vertiginous. Her gait became more unsteady, and her speech became less clear. By September of 1991, the patient had become severely dysarthric. She was unable to sustain gaze to either side, with nystagmus on lateral gaze bilaterally and slight rotatory nystagmus on upward gaze. Cranial nerves, strength, and sensory testing were otherwise normal, but the patient was ataxic on finger-to-nose and heel-to-shin testing and was unable to stand without support. An electroencephalogram was normal. An MRI scan showed slight cerebellar atrophy. Hematological studies remained normal, and urine testing for heavy metals was negative. The cerebrospinal fluid contained three cells per cubic millimeter, with normal glucose and protein levels but with one oligoclonal band. Commercial tests for anti-neuronal antibodies revealed anti-Purkinje cell antibodies. The results of an extensive search for an occult neoplasm, including mammography and ultrasonography as well as thoracic, abdominal, and pelvic computed tomography (CT), were all negative, except for slight enlargement of one adrenal gland.

Over the ensuing months, the patient's ataxia worsened and then stabilized, without improvement. CT scans showed progressive cerebellar atrophy. Mammography and pelvic MRI as well as CT studies of the chest, abdomen, and pelvis remained normal, and no change was noted in the enlarged adrenal gland. In March of 1994, however, follow-up pelvic CT suggested a mass lesion in the dome of the bladder. Cystoscopy confirmed the presence of a transitional cell carcinoma. The patient underwent laparotomy and partial resection of the bladder. A metastasis to the serosal surface of the colon was found, and the patient underwent partial colectomy. A histopathological examination of the surgical material revealed a poorly differentiated transitional cell carcinoma of the bladder (grade III), with invasion into but not through the muscularis. A similar tumor was found on the serosal surface of the colon. Extension of the tumor to regional lymph nodes was not detected. The patient has since remained neurologically unchanged, without evidence of tumor recurrence.

Materials and Methods

Patient Materials

Serum samples were obtained from the patient on August 14, 1992; February 28, 1993; June 29, 1993; March 14, 1994; October 20, 1994; and December 9, 1996. Tumor tissue was obtained as paraffin blocks from surgery. All materials were obtained under appropriate Institutional Review Board guidelines.

Immunofluorescence, Gel Electrophoresis, and Western Blot Methods

Immunofluorescence labeling of human cerebellar and brainstem sections and Western blot analysis of patient sera against Purkinje cell lysates were carried out as previously described.[1,3,4,9] Patient serum was also reacted against the CDR-62 fusion protein; cloned by Fathallah-Shaykh and coworkers[10] from a HeLa cell library using anti-Yo antibodies, this protein is considered to be a reference standard for documentation of anti-Yo autoantibody response.[3] Controls included sera from normal individuals and from patients with nonparaneoplastic neurological diseases.

Immunoperoxidase Labeling of Tumor Tissue for Expression of Anti-Yo Antigens

Sections of paraffin-embedded tissue were deparaffinized, immersed in 0.01 M of citric acid (pH 6), and microwaved for 10 minutes using the method of Cattoretti and colleagues.[11] Tissue sections were allowed to cool for 30 minutes and were then incubated with 10% normal human serum in phosphate-buffered saline for 20 minutes followed by biotinylated serum IgG from the patient for 1 hour.[12] Next, they were labeled using avidin-biotin-peroxidase complex and diaminobenzidine.[12,13] Tissue sections incubated with biotinylated serum IgG from a normal individual were used as a control. To confirm that the reactivity of the tumor was due to the expression of Yo antigens, competition assays were performed in which sections of tumor were preincubated with serum from another patient known to have anti-Yo antibodies.

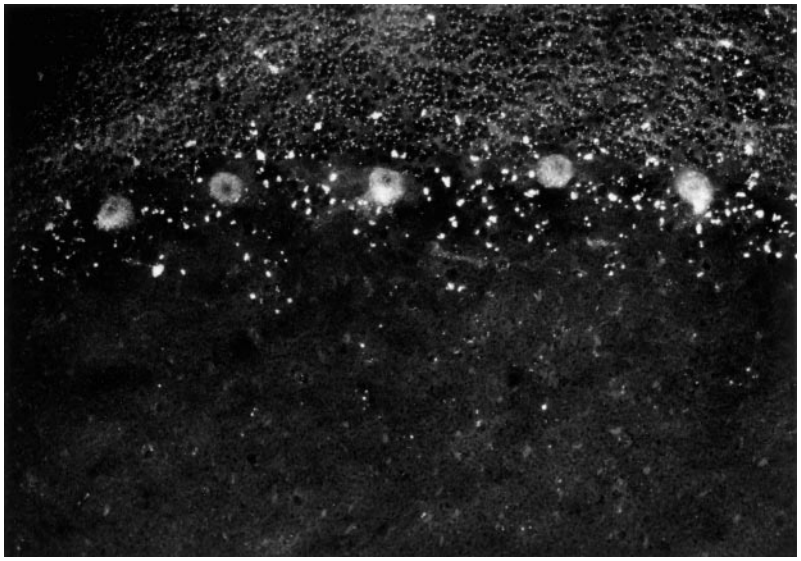

Fig 1. Patient serum diluted to a titer of 1:160 in phosphate was reacted with an acetone-fixed section of normal human cerebellum and stained using indirect immunofluorescence techniques. There is intense labeling of Purkinje cell cytoplasm with nuclear sparing, which is typical of anti-Yo antibody response (magnification ×280 before 26% reduction).

Results

Immunofluorescence and Western Blot Studies

The patient's serum produced intense immunofluorescence staining of Purkinje cell cytoplasm with sparing of Purkinje cell nuclei and reacted in Western blots with Purkinje cell proteins of 34 and 62 kd and with the CDR62 fusion protein, which is typical of anti-Yo antibody response (Figs 1 and 2). Titration of the patient's serum to end point against cerebellar sections revealed a titer of 1:5,120. Over the next 2 years, the patient's serum anti-Yo antibody titer remained within one serial dilution of this value, ranging between 1:2,560 and 1:10,240. The patient's antibody titer fell to 1:1,280 by 6 months after surgery and was 1:320 2 years later.

Fig 2. Western blot analysis of serum from Patient S125V reacted with lysate of Purkinje cell concentrate or with the CDR62 fusion protein. In both blots, P represents serum from Patient S125V, Yo represents serum from a patient previously documented to have Yo antibody response, and N represents control serum from a patient without Yo antibodies. Serum from Patient S125V (lane P) reacts with 34- and 62-kd proteins, which is characteristic of anti-Yo antibody response (exemplified by lane Yo) and labels the CDR62 fusion protein.

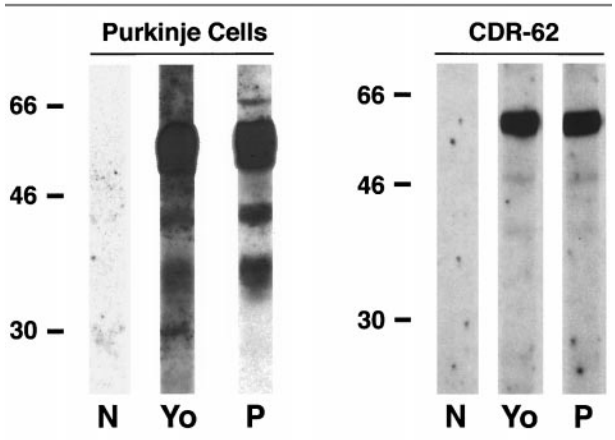

Analysis of the Patient's Tumor for Expression of Yo Antigens

The expression of Yo antigens by the tumor is demonstrated in Figure 3. Specificity of staining for Yo anti-

Fig 3. Section of the patient's tumor reacted with the patient's biotinylated IgG, which was visualized with avidin-biotin complex and diaminobenzidine and counterstained with hematoxylin. Cells within the tumor label with the biotinylated antibody (magnification ×180 before 43% reduction). The specificity of staining for the Yo antigen was confirmed by competition experiments: these demonstrated that binding of biotinylated serum IgG from the patient was blocked by preincubation of the tumor with a previously known anti-Yo serum but not with serum from a normal individual (data not shown).

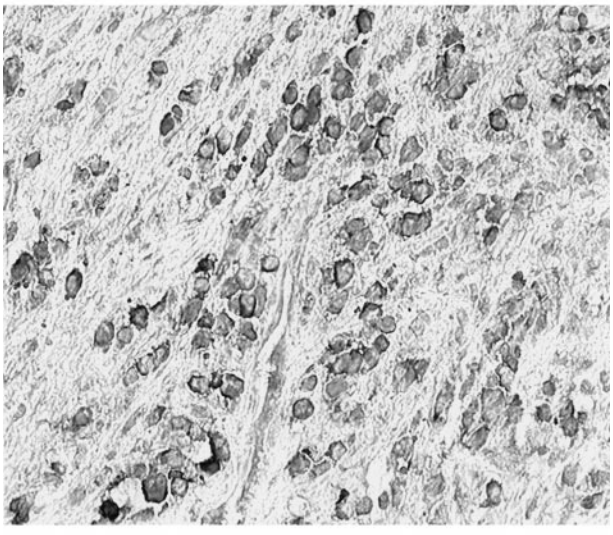

gens was confirmed by competition experiments in which binding of the biotinylated serum IgG of the patient was blocked by preincubation of tumor sections with a previously known anti-Yo serum but not with serum from a normal individual (data not shown). In addition, incubation of tumor tissue with biotinylated serum IgG from a normal individual was negative.

Discussion

Anti-Yo antibodies were first described in patients presenting with paraneoplastic cerebellar degeneration associated with adenocarcinoma of the ovary and were subsequently identified in similar patients with adenocarcinomas of the breast, uterus, and uterine adnexa.[1–3,5,14] Anti-Yo antibody response has only rarely been associated with other tumors. Hammack and coworkers[14] found ovarian malignancies in 9 of 16 patients with subacute cerebellar degeneration and antibodies to Purkinje cell cytoplasmic antigens. Fallopian tube neoplasms were found in 2 patients, endometrial carcinoma in 1 patient, ovary and breast cancer in 1 patient, and a lymphoma in 1 patient; 1 patient had an adenocarcinoma of unknown primary. In a series of 55 patients with anti-Yo antibodies, Peterson and colleagues[3] identified malignancies in 53 patients. Of these 53 patients, ovarian carcinomas were found in 26, breast carcinomas in 13, endometrial carcinomas in 4, and Fallopian carcinomas in 2. One patient had a mesovarian carcinoma, and 1 patient had an adenocarcinoma of the lung. Six patients had adenocarcinoma without known primary. Anti-Yo antibody response has been described in 2 male patients; both of these patients had gynecomastia but no definite evidence of breast malignancy.[8,15] One of these men was found to have an adenocarcinoma of unknown origin metastatic to a tracheal lymph node,[8] and the other was eventually found to have an adenocarcinoma in one parotid gland.[15]

Paraneoplastic neurological disorders in association with transitional cell carcinoma are extremely unusual. Neither Henson and Urich[16,17] in their 1982 monograph on cancer and the nervous system nor Posner[18] in his more recent text reported cases of paraneoplastic neurological injury associated with transitional cell carcinoma. Lowe and co-workers[19] have reported a case of apparent paraneoplastic brainstem encephalitis in a patient with transitional cell carcinoma of the bladder, but an association with cerebellar degeneration has not been reported. In our patient, the presence of transitional cell carcinoma was proven by tumor resection, the presence of Yo antigens within the tumor was demonstrated immunohistologically, and antibody titers fell after tumor removal. Although it is possible that she might harbor an additional breast or gynecological malignancy, no evidence of gynecological or breast carcinoma was found in this patient despite an exhaustive initial investigation, and no such malignancy has been detected despite careful follow-up over 6 years. Our findings in this patient indicate that transitional cell carcinomas of the bladder may occasionally express Yo antigens and that anti-Yo antibody response, although usually associated with gynecological and breast carcinomas, may also be found in patients with transitional cell carcinoma of the bladder. Transitional cell carcinoma should be considered in patients presenting with subacute cerebellar degeneration and anti-Yo antibody response in whom ovarian, adnexal, uterine, or breast cancer cannot be detected.

This work was supported by the United States Department of Veterans Affairs and by USPHS/NINCDS Research Award 1 R01 NS34858.

References

1. Greenlee JE, Brashear HR. Antibodies to cerebellar Purkinje cells in patients with paraneoplastic cerebellar degeneration and ovarian carcinoma. Ann Neurol 1983;14:609–613
2. Jaeckle KA, Graus F, Houghton A, et al. Autoimmune response of patients with paraneoplastic cerebellar degeneration to a Purkinje cell cytoplasmic antigen. Ann Neurol 1985;18:592–600
3. Peterson K, Rosenblum MK, Kotanides H, Posner JB. Paraneoplastic cerebellar degeneration. I. A clinical analysis of 55 anti-Yo antibody-positive patients. Neurology 1992;42:1931–1937
4. Cunningham J, Graus F, Anderson N, Posner JB. Partial characterization of the Purkinje cell antigens in paraneoplastic cerebellar degeneration. Neurology 1986;36:1163–1168
5. Greenlee JE, Brashear HR, Herndon RM. Immunoperoxidase labelling of rat brain sections with sera from patients with paraneoplastic cerebellar degeneration and systemic neoplasia. J Neuropathol Exp Neurol 1988;47:561–571
6. Hetzel D, Stanhope CR, O'Neill BP, Lennon VA. Diagnosis of gynecological cancer aided by autoimmune serological tests in patients with subacute cerebellar degeneration. Ann Neurol 1990;28:246 (Abstract)
7. Hetzel DJ, Stanhope CR, O'Neill BP, Lennon VA. Gynecological cancer in patients with subacute cerebellar degeneration predicted by anti-Purkinje cell antibodies and limited in metastatic volume. Mayo Clin Proc 1990;65:1558–1563
8. Krakauer J, Balmaceda C, Gluck JT, et al. Anti-Yo–associated paraneoplastic cerebellar degeneration in a man with adenocarcinoma of unknown origin. Neurology 1996;46:1486–1487
9. Greenlee JE, Parks TN, Jaeckle KA. Type IIa ("anti-Hu") antineuronal antibodies produce destruction of rat cerebellar granule neurons in vitro. Neurology 1993;43:2049–2054
10. Fathallah-Shaykh H, Wolf S, Wong E, et al. Cloning of a leucine-zipper protein recognized by the sera of patients with antibody-associated paraneoplastic cerebellar degeneration. Proc Natl Acad Sci USA 1991;88:3451–3454
11. Cattoretti G, Pileri S, Parravicini C, et al. Antigen unmasking on formalin-fixed, paraffin-embedded tissue sections. J Pathol 1993;171:83–98
12. Furneaux HM, Rosenblum MK, Dalmau J, et al. Selective expression of Purkinje cell antigens in tumor tissue from patients with paraneoplastic cerebellar degeneration. N Engl J Med 1990;322:1844–1851
13. Dalmau J, Furneaux HM, Cordon Cardo C, Posner JB. The expression of the Hu (paraneoplastic encephalomyelitis/sensory neuronopathy) antigen in human normal and tumor tissues. Am J Pathol 1992;141:881–886
14. Hammack JE, Kimmel DW, O'Neill BP, Lennon VA. Paraneoplastic cerebellar degeneration: a clinical comparison of patients

with and without Purkinje cell cytoplasmic antibodies. Mayo Clin Proc 1990;65:1423–1431
15. Felician O, Renard JL, Vega F, et al. Paraneoplastic cerebellar degeneration with anti-Yo antibody in a man. Neurology 1995; 45:1226–1227
16. Henson RA, Urich H. Encephalomyelitis with carcinoma. In: Cancer and the nervous system: the neurological manifestations of systemic malignant disease. Oxford: Blackwell Scientific, 1982:314–345
17. Henson RA, Urich H. Cortical cerebellar degeneration. In: Cancer and the nervous system: the neurological manifestations of systemic malignant disease. Oxford: Blackwell Scientific, 1982:346–367
18. Posner JB. Neurologic complications of cancer. Philadelpia: FA Davis, 1995
19. Lowe BA, Mershon C, Mangalik A. Paraneoplastic neurological syndrome in transitional cell carcinoma of the bladder. J Urol 1992;147:462–464

Ataxia with Isolated Vitamin E Deficiency: A Japanese Family Carrying a Novel Mutation in the α-Tocopherol Transfer Protein Gene

Masataka Hoshino, MD, Naoki Masuda, MD, PhD, Yasuhiko Ito, MD, Miho Murata, MD, PhD, Jun Goto, MD, PhD, Masaki Sakurai, MD, PhD, and Ichiro Kanazawa, MD, PhD

We report a Japanese family with ataxia with isolated vitamin E deficiency (AVED). Gene analysis revealed a single nucleotide substitution of T to C at nucleotide position 2 in the α-tocopherol transfer protein gene (*TTPA*). This substitution abolishes the start codon. The proband and his affected sister were homozygous for this mutation, and their serum α-tocopherol concentrations were remarkably reduced. Relations between the mutations and clinical features are discussed.

Hoshino M, Masuda N, Ito Y, Murata M, Goto J, Sakurai M, Kanazawa I. Ataxia with isolated vitamin E deficiency: a Japanese family carrying a novel mutation in the α-tocopherol transfer protein gene. Ann Neurol 1999;45:809–812

From the Department of Neurology, Division of Neuroscience, Graduate School of Medicine, University of Tokyo, Tokyo, Japan.

Received Oct 28, 1998, and in revised form Feb 10, 1999. Accepted for publication Feb 19, 1999.

Address correspondence to Dr Goto, Department of Neurology, Division of Neuroscience, Graduate School of Medicine, University of Tokyo, 7-3-1 Hongo, Bunkyo-ku, Tokyo 113-8655, Japan.

Ataxia with isolated vitamin E deficiency (AVED; MIM 277460) is a progressive neurodegenerative disease characterized by locomotor ataxia, hyporeflexia, and decreased proprioceptive sensation. Although there are neurophysiological and pathological differences, these clinical features are strikingly similar to those of Friedreich's ataxia.[1–7] In addition, some patients have accompanying retinitis pigmentosa. The disease is inherited in an autosomal recessive manner, and the underlying biochemical defect is the impairment of α-tocopherol incorporation into very low density lipoprotein in the liver.[8,9] The α-tocopherol transfer protein functions in that incorporation. The gene (*TTPA*) for this protein is located on chromosome 8q13. Its mutation has been shown to cause AVED; to date, 15 different mutations of *TTPA* have been identified in AVED patients in North Africa, Europe, North America, and Japan.[1–6] We report a novel mutation identified in a Japanese family with AVED.

Family

Patient 1 (IV-1)

The proband, a 41-year-old man (Fig 1), was the firstborn child of a consanguineous marriage (III-5 and III-11). The parents were first cousins. He experienced unsteadiness of gait at the age of 15 years. Difficulty in speech and visual impairment appeared at the age of 19 years. Since he was approximately 27 years old, he has had to use a cane for walking. His mental functions were normal, but his visual acuity was severely impaired, and he could scarcely count his fingers. An ophthalmological examination detected the bilateral central type of retinitis pigmentosa. His speech was slightly slurred. There was a moderate degree of ataxia in all four limbs and the trunk. Deep tendon reflexes were absent generally, but plantar responses were extensor bilaterally. His gait was wide-based and unsteady. Vibratory sense was lost in the forearms and lower limbs, position sense was moderately

Fig 1. Family pedigree. Square symbols *represent male members, and* circles *represent female members.* Filled symbols *represent neurological symptoms, the* half-filled symbol *represents a carrier, the* half-crosshatched symbol *represents an obligate carrier,* diagonal lines *represent deceased individuals, and the* arrow *represents the proband. Concentrations of serum α-tocopherol are shown in parentheses.*

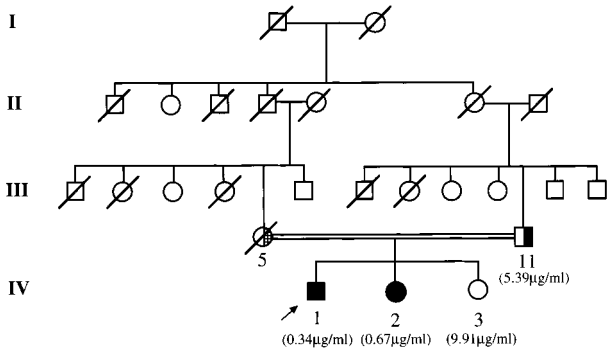

reduced in the feet, and Romberg's sign was positive. The serum α-tocopherol concentration was 0.34 mg/ml (normal, 5.7–14.3 μg/ml), although the serum vitamin A–, vitamin D–, and vitamin K–dependent coagulation studies and betalipoprotein were normal, and serum phytanic acid was not detected. An orally administered test of α-tocopherol acetate showed a normal increase in the serum vitamin concentration but an accelerated decrease in the serum vitamin concentration.

Patient 2 (IV-2)

This 40-year-old woman was the younger sister of the proband (see Fig 1). Although she noticed no difficulties herself, a neurological examination showed mild unsteadiness during tandem walking and when standing on one foot. Position sense was preserved, but vibration sense was impaired, and deep tendon reflexes were reduced. No sign of retinitis pigmentosa was detected. Her serum α-tocopherol concentration was 0.67 μg/ml.

Other Family Members

The father (III-11) and youngest sister (IV-3) showed no neurological abnormalities. Their respective serum α-tocopherol concentrations were 5.39 and 9.91 μg/ml.

Materials and Methods

Polymerase Chain Reaction Amplification of Genomic DNA

Genomic DNA was extracted from peripheral blood leukocytes by the standard method.[10] *TTPA* consists of five exons. The primer pairs used to amplify the exons by polymerase chain reaction (PCR) were as follows:

Exon 1: TTAAGAGGCAGCTCTGCTCG and CTTCGGCAGGGGTCAGATAT
Exon 2: CCATGTATGCCATTTGTAGAC and GGGAACACAACTGAACTGGA
Exon 3: CACAATGCTAAGATATGATATGC and GGAAGTATTATGGCTGACAGT
Exon 4: ACTTGACATTAGGTATCAGATT and TGTTTGGTGTAGAGGAACAC
Exon 5: CATCTAATGCGGTTTCCTTC and TTTAGTTAGGAAGCCATTCACA

Conditions for PCR amplification of exon 1 were 35 cycles consisting of 1 minute at 95°C, 1 minute at 57°C, and 1 minute at 73°C. The thermal cycle reactions were preceded by denaturation at 95°C for 12 minutes. Conditions for PCR amplification of exons 2, 3, 4, and 5 were 30 cycles consisting of 1 minute at 95°C, 2 minutes at 55°C, and 1 minute at 73°C. The preceding denaturation was 3 minutes at 95°C. PCR products were purified by agarose gel electrophoresis and used for direct sequencing. They also were subcloned using the pGEM-T Easy vector (Promega, Madison, WI).

Nucleotide Sequencing

Sequencing was done using an automated fluorescence sequencer (ABI 377; Perkin Elmer, Foster City, CA).

Results

To investigate the possibility of mutation in *TTPA*, PCR was done on the genomic DNA of the proband. The sequence obtained showed a single nucleotide substitution: a T-to-C transition at the second position of the start codon in exon 1 (Fig 2). This substitution causes abolition of the translation start site. The proband was homozygous for the mutation. The same mutation was confirmed in his sister (IV-2) on sequencing her PCR products, and she also was homozygous. Their father (III-11) was a heterozygote for the mutant and normal alleles.

Discussion

The main clinical features of this family were ataxia, a decrease in deep sensations, hypo- or areflexia, and retinitis pigmentosa. Serum vitamin E concentrations were abnormally low in the affected members: the proband (IV-1) and 1 of his sisters (IV-2). Clinical and laboratory data indicated the diagnosis of AVED and excluded secondary vitamin E deficiencies such as chronic fat malabsorption, abetalipoproteinemia, and Friedreich's ataxia. To determine whether a mutation causes AVED, we sequenced all five exons of *TTPA*. The mutation common to this family was a single nucleotide substitution of T to C at nucleotide position 2, which abolishes the start codon and presumably results in abortion of the translation of the mutant allele. Both patients were homozygous for the mutation. Fifteen mutations in *TTPA* have been reported in patients from 33 AVED families.[1–6] The Table shows the relationships between the genotypes and clinical features of these and our patients.[1–6,11–16] In most of these families, the patients were homozygotes for mutant alleles, but compound heterozygotes for different mutations have been described in 4 families. In AVED patients, biochemical study results show that the severity of neurological dysfunction depends on the type of defect in the transfer protein and on vitamin E supplementation.[8,9] Cavalier and co-workers[6] analyzed the phenotypic variability of 13 mutations in 29 families. They classified the families into 3 groups based on the types of mutations: families in which the patients had truncating mutations (frameshift and nonsense) and those in which the patients had nonconservative missense mutations or semiconservative missense mutations. In the first and second groups, the respective mean ages at disease onset were 9 and 10 years, whereas in the third group, the mean age at disease onset was 29 years, which provides evidence of a correlation between genotype and severity in AVED. The mutation described in this report abolishes the start codon, and, presumably, no α-tocopherol transfer protein is produced in the homozygous patients. The ages at disease onset of our patients, however, were older than those of patients

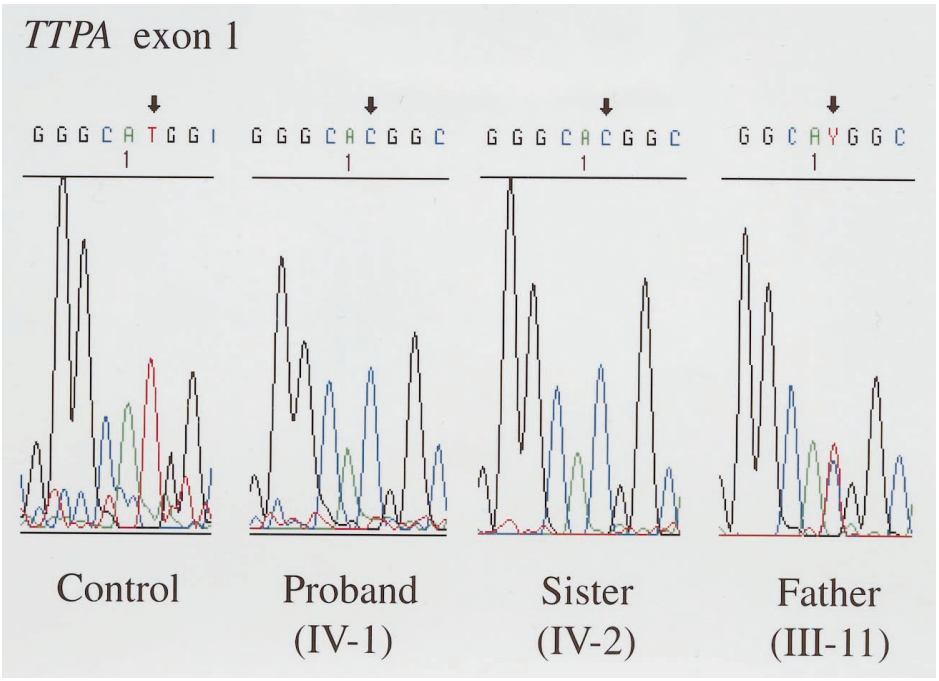

Fig 2. Direct sequencing of polymerase chain reaction–amplified products from exon 1 of the α-tocopherol transfer protein gene. Arrows *indicate the mutation site, and* Y *indicates pyrimidine nucleotides C and T.*

Table. Mutations and Clinical Findings in Ataxia with Isolated Vitamin E Deficiency

Mutation				Clinical Findings									
Position													
Exon	Nucleotide	Type	Effect	Number of Patients	Age at Onset (yr)	Ataxia[a]	Hyporeflexia[a]	Dysarthria[a]	Disturbance of Proprioception[a]	Disturbance of Vibratory Sense[a]	Pigmentary[a] Retinopathy	Vitamin E (μg/ml)	Reference[d]
Homozygote													
Exon 1	2	T to C	Abolishing start codon	IV-1[b]	15	1	1	1	1	1	1	0.34	This report
				IV-2[b]	40	1	1	0	0	1	0	0.67	This report
Truncating													
Exon 3	400	C to T	Nonsense	1	5	1	1	—	1	1	0	<1.0	6
	486	1-bp deletion	Frameshift	2	7–8	2	2	2	1/1	1	0	<1.1	2,6
	513	2-bp insertion	Frameshift	2	3–5	2	2	2	1/1	2	0	<1.0–<2.1	2,6
	530	AG to GTAAGT	Frameshift	1	3	1	1	1	1	1	0	<1.0	1,6
	552	G to A	Exon skipping	1	<10	1	1	0	1	1	0	1.2	4
Exon 5	744	1-bp deletion	Frameshift	20	3–19	20	20	16	8/10	18	1/19	0.25–2.0	1,6,11,12,14
Subtotal				27	—	27	27	21	13	24	1		
Missense													
Exon 1	175	C to T	R59W/ R59W	1	7	1	1	1	—	1	0	0.3	6
Exon 2	303	T to G	H101Q/ H101Q	5	30–<70	4/4	5	4/4	5	5	2/4	1.0–3.2	6,15,16
	358	G to A	A120T/ A120T	1	21	1	1	0	—	1	1[c]	1.0	6
Exon 3	421	G to A	E141K/ E141K	1	8	1	1	1	—	1	0	1.3	6
Exon 4	566	T to C	L183P/ L183P	1	—	1	1	1	1	1	1	1.7	5
	661	C to T	R221W/ R221W	3	10–14	3	—	—	—	0	—	—	6
Subtotal				12	—	11	9	7	6	9	4	—	
Heterozygote													
Exon 2	306	A to G	Aberrant splicing										
and				2	16	2	0	1	—	2	0	1.2–3.3	6
Exon 3	513	2-bp insertion	Frameshift										
Exon 2	205-1	G to C	Aberrant splicing										
and				1	2	1	1	1	—	1	1[c]	1.2	6
Exon 5	744	1-bp deletion	Frameshift										
Exon 3	400	C to T	Nonsense										
and	486	1-bp deletion	Frameshift	1	6	1	1	1	—	1	0	<2.0	6
Exon 3	513	2-bp insertion	Frameshift										
and				3	6–<27	1	0	0	1	3	0	1.2–1.8	2,6,13
Exon 4	574	G to A	R192H										
Subtotal				7		5	2	3	1	7	1		
Total				48		45	40	32	21	42	7		

[a]Indicates the number of patients presenting this symptom. The denominator is the number of patients for whom clinical information is available.
[b]Patient numbers given are according to this report.
[c]Retinopathy is not apparent, but moderately reduced amplitudes are present on the electroretinogram.
[d]Not all clinical reports were cited. They can be referred to mutation reports.

homozygous for the 744delA mutation, which is the most frequent truncating mutation. Moreover, there is a marked difference in the clinical findings for our proband and his sister, including the age at disease onset and severity of ataxia, irrespective of their having the same mutation. The proband showed retinitis pigmentosa, and this is also associated with two other Japanese missense mutations.[5,16] Retinopathy is relatively rare among patients with AVED of other ethnic stocks, however.[14,17,18] Our patients have been given a vitamin E supplement. A high oral dose of vitamin E is reported to stabilize or lessen neurological deterioration in AVED patients, especially in pre- or paucisymptomatic patients.[2,3,11,13,14,16–18] These molecular findings and clinical observations suggest that in addition to genotype, factors such as ethnic or genetic background and dietary factors profoundly affect the clinical features of AVED.

References

1. Ouahchi K, Arita M, Kayden H, et al. Ataxia with isolated vitamin E deficiency is caused by mutations in the α-tocopherol transfer protein. Nat Genet 1995;9:141–145
2. Hentati A, Deng H-X, Hung W-Y, et al. Human α-tocopherol transfer protein: gene structure and mutations in familial vitamin E deficiency. Ann Neurol 1996;39:295–300
3. Gotoda T, Arita M, Arai H, et al. Adult-onset spinocerebellar dysfunction caused by a mutation in the gene for the α-tocopherol–transfer protein. N Engl J Med 1995;333:1313–1318
4. Tamaru Y, Hirano M, Kusaka H, et al. α-Tocopherol transfer protein gene: exon skipping of all transcripts causes ataxia. Neurology 1997;49:584–588
5. Shimohata T, Date H, Ishiguro H, et al. Ataxia with isolated vitamin E deficiency and retinitis pigmentosa. Ann Neurol 1998;43:273
6. Cavalier L, Ouahchi K, Kayden HJ, et al. Ataxia with isolated vitamin E deficiency: heterogeneity of mutations and phenotypic variability in a large number of families. Am J Hum Genet 1998;62:301–310
7. Zouari M, Feki M, Ben Hamida C, et al. Electrophysiology and nerve biopsy: comparative study in Friedreich's ataxia and Friedreich's ataxia phenotype with vitamin E deficiency. Neuromusc Disord 1998;8:416–425
8. Traber MG, Sokol RJ, Burton GW, et al. Impaired ability of patients with familial isolated vitamin E deficiency to incorporate α-tocopherol into lipoproteins secreted by the liver. J Clin Invest 1990;85:397–407
9. Traber MG, Sokol RJ, Kohlschütter A, et al. Impaired discrimination between stereoisomers of α-tocopherol in patients with familial isolated vitamin E deficiency. J Lipid Res 1993;34:201–210
10. Sambrook J, Fritsch EF, Maniatis T. Molecular cloning: a laboratory manual. 2nd ed. New York: Cold Spring Harbor Laboratory Press, 1989
11. Ben Hamida M, Belal S, Sirugo G, et al. Friedreich's ataxia phenotype not linked to chromosome 9 and associated with selective autosomal recessive vitamin E deficiency in two inbred Tunisian families. Neurology 1993;43:2179–2183
12. Ben Hamida C, Doerflinger N, Belal S, et al. Localization of Friedreich ataxia phenotype with selective vitamin E deficiency to chromosome 8q by homozygosity mapping. Nat Genet 1993;5:195–200
13. Sokol RJ, Kayden HJ, Bettis DB, et al. Isolated vitamin E deficiency in the absence of fat malabsorption–familial and sporadic cases: characterization and investigation of causes. J Lab Clin Med 1988;111:548–559
14. Amiel J, Maziere JC, Beucler I, et al. Familial isolated vitamin E deficiency. Extensive study of a large family with a 5-year therapeutic follow-up. J Inherit Metab Dis 1995;18:333–340
15. Yokota T, Wada Y, Furukawa T, et al. Adult-onset spinocerebellar syndrome with idiopathic vitamin E deficiency. Ann Neurol 1987;22:84–87
16. Yokota T, Shiojiri T, Gotoda T, et al. Friedreich-like ataxia with retinitis pigmentosa caused by the $His^{101}Gln$ mutation of the α-tocopherol transfer protein gene. Ann Neurol 1997;41:826–832
17. Rayner RJ, Doran R, Roussounis SH. Isolated vitamin E deficiency and progressive ataxia. Arch Dis Child 1993;69:602–603
18. Shorer Z, Parvari R, Bril G, et al. Ataxia with isolated vitamin E deficiency in four siblings. Pediatr Neurol 1996;15:340–343

A Novel Phenotype in Familial Creutzfeldt-Jakob Disease: Prion Protein Gene E200K Mutation Coupled with Valine at Codon 129 and Type 2 Protease-Resistant Prion Protein

Johannes A. Hainfellner, MD,* Piero Parchi, MD,† Tetsuyuki Kitamoto, MD,‡ Christa Jarius, MD,* Pierluigi Gambetti, MD,† and Herbert Budka, MD*

A novel phenotype of familial Creutzfeldt-Jakob disease (CJD) with mutated codon 200 of the prion protein gene (*PRNP*) coupled with the valine codon 129 (E200K-129V haplotype) has two features never observed in subjects carrying the pathogenic mutation coupled with the methionine codon 129 (E200K-129M haplotype): (1) plaque-like prion protein (PrP) deposits in the cerebellum and (2) type 2 protease-resistant prion protein (PrP^{res}). This observation further underlines the role of codon 129 on the mutated *PRNP* allele in modulating the phenotype of familial prion diseases.

From the *Institute of Neurology, University of Vienna, and the Austrian Reference Center for Human Prion Diseases, Vienna, Austria; †Division of Neuropathology, Institute of Pathology, Case Western Reserve University, Cleveland, OH; and ‡Department of Neurological Science, Tohoku University, Sendai, Japan.

Received Aug 27, 1998, and in revised form Feb 24, 1999. Accepted for publication Feb 26, 1999.

Address correspondence to Prof Budka, Institute of Neurology, AKH, Währinger Gürtel 18-20, POB 48, A-1097 Vienna, Austria.

Hainfellner JA, Parchi P, Kitamoto T, Jarius C, Gambetti P, Budka H. A novel phenotype in familial Creutzfeldt-Jakob disease: prion protein gene E200K mutation coupled with valine at codon 129 and type 2 protease-resistant prion protein. Ann Neurol 1999;45:812–816

One fascinating feature of prion diseases is the range of clinical and pathological characteristics and the complexity of the genotype-phenotype relationship in inherited forms. The disease phenotype linked to the mutation at codon 178 (D178N) of the prion protein gene (*PRNP*) changes radically according to the genotype of codon 129, the site of a methionine-valine polymorphism.[1,2] Much less is known concerning the role of codon 129 in other *PRNP* mutations. Alternative coupling of the pathogenic mutation with the methionine or valine codon 129 (129M or 129V haplotype) has also been reported in the P102L point mutation as well as in the four- and five-repeat insertion mutations.[3,4]

To date, the E200K mutation, the most common *PRNP* mutation, has been reported only in coupling with the methionine codon 129.[5–10] The phenotype linked to the E200K-129M haplotype strongly resembles that of typical sporadic Creutzfeldt-Jakob disease (CJD) and is invariably associated with protease-resistant prion protein (PrP^{res}) type 1.[5–12] We now report for the first time the coupling of the *PRNP* E200K mutation with valine at codon 129 and PrP^{res} type 2. Several associated phenotypic features have never been observed in CJD linked to the E200K-129M haplotype. This unique observation provides the opportunity to further assess the role of codon 129 in determining clinical, pathological, and PrP^{res} features in inherited prion diseases.

Methods and Results

Pedigree

In Generation II, all 6 siblings died between the ages of 50 and 65 years with descriptions of dementia or depression of undetermined cause; Siblings II:2 and II:4 committed suicide (Fig 1). The proband's sisters (III:2 and III:3) are healthy at the ages of 65 and 67 years, respectively.

Genotype

High-molecular-weight DNA was extracted from frozen brain tissue of the proband (III:1) and from peripheral blood cells of the proband's daughter (IV:1). Polymerase chain reaction (PCR) amplification of *PRNP* was performed with primers T-1 (GATGCTGGTTCTCTTTGTGG) and T-2 (CCCACTATCAGGAAGATGAG). Restriction fragment length polymorphism with Dde I, Alu I, Pvu II, NspI, Mae I, Tth111 I, Bsm AI, Spl I, and Nla III screened for mutations or polymorphism of codons 102, 105, 117, 129, 145, 178/180, 200, 219, and 232, respectively.[13] In the proband, restriction fragment length polymorphism identified valine homozygosity at codon 129 (V129V) and a heterozygous codon 200 glutamate-to-lysine (E200K) mutation; polymorphic codon 219 was homozygous for glutamic acid (Fig 2A). For direct PCR sequencing, the complete open reading frame of *PRNP* was amplified with primers P-1 (AAGAATTCTCTGACATTCTCCTCTTCA) and P-2 (AAGGATCCCTCAAGCTGGAAAAG). PCR products were sequenced by the ABI 377 DNA sequencer with the dye-terminator FS kit (Perkin Elmer, Norwalk, CT). Sequence analysis confirmed the presence of the E200K mutation and excluded other mutations. The octapeptide repeat region[14] did not harbor deletion polymorphism. No mutation was detected in the proband's daughter.

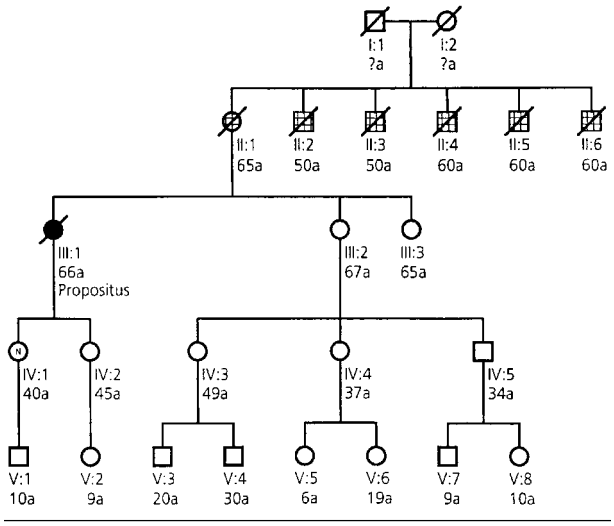

Fig 1. Pedigree of the Austrian Creutzfeldt-Jakob disease (CJD) family with the prion protein gene (PRNP) *E200K mutation.* Circles *indicate female members, and* squares *indicate male members; a* diagonal bar *in the symbols signifies deceased family members. Generations are indicated with* roman numerals, *and* arabic numerals *identify individuals within each generation.* Crosshatched symbols *(Members II: 1–II:6) have probable CJD according to nonmedical data. The* dark symbol *(proband) indicates the* PRNP *E200K mutation as proven by genomic analysis; the* circle containing an N *(Member IV:1) indicates that genomic analysis revealed normal* PRNP.

Proband's Phenotype

CLINICAL HISTORY. This 66-year-old woman presented with a 2.5-year history of slight memory impairment and a 1-year history of intermittent "swaying" vertigo. Three and one-half months before her death,

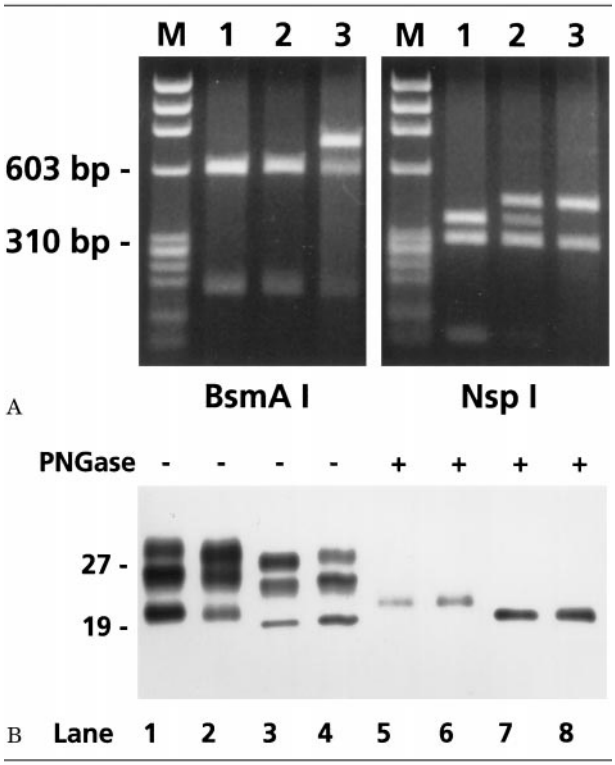

Fig 2. Molecular genetic and Western blot analyses. (A) BsmAI cutting shows the pattern of wild-type patients in lanes 1 and 2; lane 3 (proband) shows the pattern of the prion protein gene E200K mutation. NsPI cutting reveals codon 129 polymorphism: lane 1 shows the pattern of M129M, lane 2 shows that of M129V, and lane 3 shows that of V129V (proband). (B) Western blot of proteinase K–treated brain homogenates from subjects with sporadic Creutzfeldt-Jakob disease (CJD) types 1 and 2, and CJD[200] types 1 and 2 before (lanes 1–4) and after (lanes 5–8) deglycosylation. All samples were obtained from the cerebral cortex. Lanes 1 and 5: sporadic CJD, M129M, protease-resistant prion protein (PrP^{res}) type 1; lanes 2 and 6: CJD E200K, M129M, PrP^{res} type 1; lanes 3 and 7 (proband): CJD E200K, V129V, PrP^{res} type 2; lanes 4 and 8: sporadic CJD, V129V, PrP^{res} type 2.

dementia was noticed and progressed rapidly. She was neurologically examined when she was already confined to bed. Disorientation (eg, personal identity, time, place), dysarthria, slight spasticity, and slightly increased deep tendon reflexes of the upper extremities were found. There was no myoclonus. Laboratory tests, including cerebrospinal fluid examination, were unremarkable. An electroencephalogram showed diffuse slowing and right frontal triphasic spikes. Computed tomography and cerebral magnetic resonance imaging revealed ventricular enlargement. Single-photon emission computed tomography with ^{99m}Tc-bicisate (neurolite) disclosed hypoperfusion in the right frontoparietotemporal lobes. She died severely demented in a nursing home.

NEUROPATHOLOGY. A postmortem brain examination revealed slight to moderate diffuse cerebral and cerebellar atrophy. Diffuse spongiform degeneration, astrogliosis, and neuronal loss occurred in cerebral and cerebellar cortices and basal ganglia. Cerebellar Purkinje and granular cells were moderately reduced, and torpedoes were present. Immunocytochemistry showed diffuse small granular (synaptic type) prion protein (PrP) deposits in cerebral cortex, basal ganglia, brainstem, and cerebellar cortex. In addition, unicentric plaque-like PrP deposits occurred in the cerebellar granular cell layer and subcortical white matter (Fig 3). These deposits did not stain with Congo red. Slight to moderate neurofibrillary degeneration was detectable in the hippocampus and parahippocampus (stage II according to Braak and Braak[15]).

IMMUNOBLOT ANALYSIS OF PrP^{res}. Frozen frontal cortex, striatum, and cerebellum were processed as previously described.[11] In each region, immunoblots showed the presence of PrP^{res}, consisting of three major peptides with electrophoretic mobilities of approximately 28, 26, and 19 kd. Deglycosylation resulted in a single band of approximately 19 kd, indicating that the 28- and 26-kd peptides correspond to distinct PrP^{res} glycoforms (see Fig 2B). The electrophoretic mobility of PrP^{res} in the proband represented PrP^{res} type 2, which has been described previously in sporadic CJD and fatal familial insomnia (FFI).[11,12] The stoichiometry among the PrP^{res} bands corresponding to the diglycosylated, monoglycosylated, and unglycosylated forms, which provide an additional means to characterize PrP^{res}, was 1:0.74:0.39 similar to that of PrP^{res} type 1 associated with the E200K-129M haplotype (P. Parchi and P. Gambetti, unpublished data, 1998). Quantitative analysis showed a higher quantity of PrP^{res} in the cerebellum than in the frontal cortex (data not shown).

Discussion

The present observation allows for a comparative analysis of the characteristics associated with the two haplotypes linked to CJD[200]: the common E200K-129M haplotype and the E200K-129V haplotype. The clinical features associated with the former resemble those of typical sporadic CJD. In the proband, disease onset and duration are difficult to assess. A 2.5-year history of slight memory impairment is likely to represent incipient Alzheimer's disease rather than early CJD, because neuropathology showed transentorhinal Alzheimer-type neurofibrillary degeneration. Although ataxia could not be evaluated on neurological examination because the patient was already severely demented and bedridden, it is likely that the described "vertigo" was in fact ataxia. The rapidly progressive dementia of 3.5 months' duration was not accompanied by myoclonus.

The histopathology of the E200K-129M haplotype

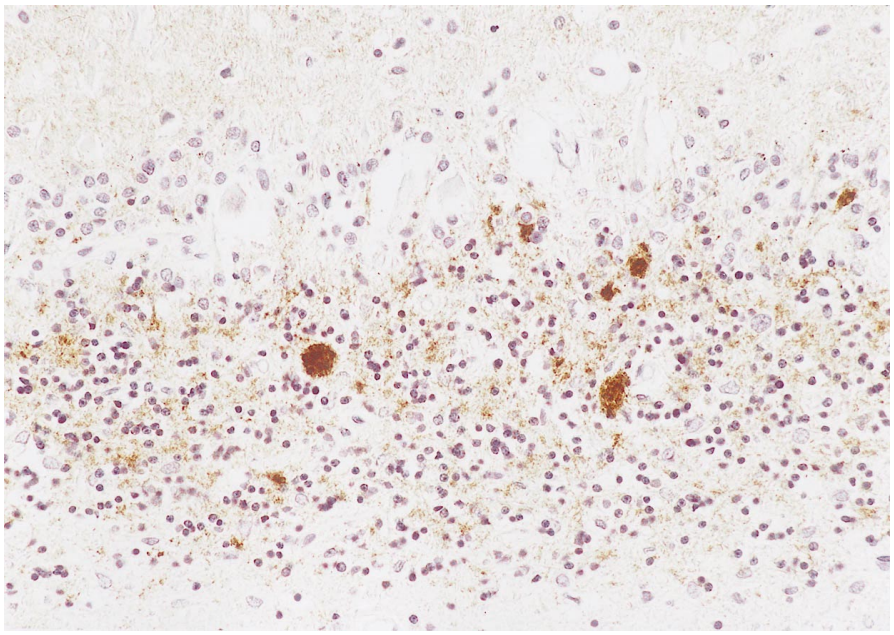

Fig 3. Anti-prion protein (PrP) immunohistochemistry. Cerebellar cortex with diffuse synaptic type PrP deposits and plaque-like PrP deposits in granular cell layer (magnification ×190 before 7% reduction).

also strongly resembles that of typical sporadic CJD. E200K-129M cases show spongiosis, gliosis, and neuronal loss mainly affecting the cerebral cortex, striatum, thalamus, and cerebellum, without amyloid plaques. PrP immunocytochemistry[9,10] (as well as P. Parchi and P.Gambetti, unpublished data, 1998) reveals a punctate and synaptic type of staining in gray matter. Widespread spongiosis and PrP^{res} deposition of synaptic type were also found in the proband. In addition, however, the cerebellar cortex contained unicentric plaque-like PrP deposits. Immunoblot analyses disclosed PrP^{res} of type 2 according to Parchi and co-workers[11] as opposed to the PrP^{res} type 1 observed in all CJD cases with the E200K-129M haplotype examined to date[9] (as well as P. Parchi and P. Gambetti, unpublished data, 1998). Therefore, the phenotype associated with the E200K-129V haplotype definitely appears to differ for (1) the presence of nonamyloid plaques and (2) the lower relative molecular mass (*M*r) of the PrP^{res} fragment generated by treatment with proteinase K.

The effect of codon 129 on the phenotype linked to the E200K mutation seems to be less striking than that observed in the D178N and P102L mutations. The former is linked to FFI, characterized by insomnia and dysautonomia associated with thalamic atrophy, when the methionine codon is present at position 129 of the mutant allele.[1] In contrast, the D178N mutation is linked to a CJD phenotype (CJD^{178}) when coupled with the valine codon 129. Moreover, although PrP^{res} in FFI has an *M*r of 19 kd after deglycosylation, corresponding to PrP^{res} type 2, the *M*r of the PrP^{res} present in CJD^{178} is 21 kd, corresponding to PrP^{res} type 1.[2,11] When coupled with the P102L mutation, codon 129 also affects the phenotype of Gerstmann-Sträussler-Scheinker disease.[3] Compared with Gerstmann-Sträussler-Scheinker patients with the common P102L-129M haplotype,[16] the subject with the P102L-129V haplotype had a longer disease course, seizures, and long tract signs with no dementia, and the pathology was remarkable for a lack of spongiosis and for significant involvement of the spinal cord. The PrP^{res} type associated with the P102L-129V haplotype has not been reported.[3] As for the four- and five-repeat insertion mutations, only the age at onset and the disease duration have been recorded and found to vary as a function of codon 129.[4]

The mechanism by which codon 129 modulates the disease phenotype associated with the *PRNP* mutation has not been definitely established but seems to relate to a synergistic effect on the conformation of the mutant PrP^{res}. This hypothesis was recently strengthened by two significant findings. First, although there is no direct contact, the side chains of PrP residues 129 and 178 are connected by a hydrogen bond that could mediate interactions between these two residues.[17] Second, to date, alternative coupling of the same *PRNP* mutation with either the methionine or valine codon 129 has always led to the expression of a different PrP^{res} type; each type is believed to represent a conformationally distinct PrP^{res} isoform.[2,18] Therefore, codon 129 would modify the effect that the pathogenic *PRNP* mutation has on the conformation of the mutant PrP. In turn, conformationally different mutant PrP would convert into PrP^{res} isoforms that also differ in conformation and cause distinct disease phenotypes.

The modulating effect on conformation of the inter-

play between a mutant and homoallelic polymorphic residue exemplified in the present report provides a simple explanation for phenotypic heterogeneity of inherited prion diseases. A similar mechanism might operate in other inherited disorders.

This study is part of the European Union Biomed-2 Concerted Action "Human Transmissible Spongiform Encephalopathies (Prion Diseases): Neuropathology and Phenotypic Variation" project (Dr Budka is the project leader).

References

1. Goldfarb LG, Petersen RB, Tabaton M, et al. Fatal familial insomnia and familial Creutzfeldt-Jakob disease: disease phenotype determined by a DNA polymorphism. Science 1992;258: 806–808
2. Monari L, Chen SG, Brown P, et al. Fatal familial insomnia and familial Creutzfeldt-Jakob disease: different prion proteins determined by a DNA polymorphism. Proc Natl Acad Sci USA 1994;91:2839–2842
3. Young K, Clark HB, Piccardo P, et al. Gerstmann-Sträussler-Scheinker disease with the *PRNP* P102L mutation and valine at codon 129. Mol Brain Res 1997;44:147–150
4. Baker HF, Poulter M, Crow TJ, et al. Amino acid polymorphism in human prion protein and age at death in inherited prion disease. Lancet 1991;337:1286 (Letter)
5. Antoine JC, Laplanche JL, Mosnier JF, et al. Demyelinating peripheral neuropathy with Creutzfeldt-Jakob disease and mutation at codon 200 of the prion protein gene. Neurology 1996; 46:1123–1127
6. Collinge J, Palmer MS, Campbell T, et al. Inherited prion disease (PrP lysine 200) in Britain: two case reports. BMJ 1993; 306:301–302
7. Gabizon R, Rosenman H, Meiner Z, et al. Mutation in codon 200 and polymorphism in codon 129 of the prion protein gene in Libyan Jews with Creutzfeldt-Jakob disease. Philos Trans R Soc Lond B Biol Sci 1994;343:385–390
8. Salvatore M, Pocchiari M, Cardone F, et al. Codon 200 mutation in a new family of Chilean origin with Creutzfeldt-Jakob disease. J Neurol Neurosurg Psychiatry 1996;61:111–112 (Letter)
9. Inoue I, Kitamoto T, Doh-ura K, et al. Japanese family with Creutzfeldt-Jakob disease with codon 200 point mutation of the prion protein gene. Neurology 1994;44:299–301
10. Kitamoto T, Doh-ura K, Muramoto T, et al. The primary structure of the prion protein influences the distribution of abnormal prion protein in the central nervous system. Am J Pathol 1992;141:271–277
11. Parchi P, Castellani R, Capellari S, et al. Molecular basis of phenotypic variability in sporadic Creutzfeldt-Jakob disease. Ann Neurol 1996;39:767–778
12. Parchi P, Capellari S, Chen SG, et al. Typing prion isoforms. Nature 1997;386:232–234
13. Kitamoto T, Tateishi J. Human prion diseases with variant prion protein. Philos Trans R Soc Lond B Biol Sci 1994;343: 391–398
14. Palmer MS, Mahal SP, Campbell TA, et al. Deletions in the prion protein gene are not associated with CJD. Hum Mol Genet 1993;2:541–544
15. Braak H, Braak E. Neuropathological staging of Alzheimer-related changes. Acta Neuropathol (Berl) 1991;82:239–259
16. Hainfellner JA, Brantner Inthaler S, Cervenakova L, et al. The original Gerstmann-Sträussler-Scheinker family of Austria: divergent clinicopathological phenotypes but constant PrP genotype. Brain Pathol 1995;5:201–211
17. Riek R, Wider G, Billeter M, et al. Prion protein NMR structure and familial human transmissible spongiform encephalopathies. Proc Natl Acad Sci USA 1998;95:11667–11672
18. Telling GC, Parchi P, DeArmond SJ, et al. Evidence for the conformation of the pathologic isoform of the prion protein enciphering and propagating prion diversity. Science 1996;274: 2079–2082

Relation of JC Virus DNA in the Cerebrospinal Fluid to Survival in Acquired Immunodeficiency Syndrome Patients with Biopsy-Proven Progressive Multifocal Leukoencephalopathy

Constantin T. Yiannoutsos, PhD,*
Eugene O. Major, PhD,† Blanche Curfman, BA,†
Peter N. Jensen, BS,† Maneth Gravell, PhD,†
Jean Hou, BA,† David B. Clifford, MD,‡
and Colin D. Hall, MB ChB§

The detection and semiquantitation of JC virus (JCV) DNA in cerebrospinal fluid (CSF) is prognostic of survival and is a marker of the course of progressive multifocal leukoencephalopathy (PML). CSF samples from 15 acquired immunodeficiency syndrome (AIDS) patients with biopsy-proven PML were analyzed by semiquantitative polymerase chain reaction (PCR). A low JCV burden was predictive of longer survival compared with a high JCV burden (median survival from entry, 24 [2–63] vs 7.6 [4–17] weeks). Further analyses indicated a possible threshold of 50 to 100 copies/μl separating high- and moderate-risk cases. Patients with a JCV load below this level survived longer than those with a JCV load above it.

From the *Center for Biostatistics in AIDS Research, Harvard School of Public Health, Boston, MA; †Laboratory of Molecular Medicine and Neuroscience, National Institute of Neurological Disorders and Stroke, Bethesda, MD; ‡Department of Neurology, Washington University School of Medicine, St Louis, MO; and §Department of Neurology, University of North Carolina School of Medicine, Chapel Hill, NC.

Received Dec 8, 1998, and in revised form Feb 15, 1999. Accepted for publication Feb 26, 1999.

Address correspondence to Dr Yiannoutsos, Center for Biostatistics in AIDS Research, Harvard School of Public Health, 651 Huntington Avenue, Boston, MA 02115-6017.

Yiannoutsos CT, Major EO, Curfman B, Jensen PN, Gravell M, Hou J, Clifford DB, Hall CD. Relation of JC virus DNA in the cerebrospinal fluid to survival in acquired immunodeficiency syndrome patients with biopsy-proven progressive multifocal leukoencephalopathy. Ann Neurol 1999;45:816–821

Progressive multifocal leukoencephalopathy (PML) is a devastating neurological disease resulting from JC virus (JCV) infection.[1,2] Described in immunosuppressed patients with malignancies, PML is increasingly seen among human immunodeficiency virus (HIV) patients. Median survival ranges from 2 to 6 months after the onset of symptoms[3–5] and slightly longer if PML is the acquired immunodeficiency syndrome (AIDS)–defining illness.[6,7] Up to 10% of patients show prolonged survival, irrespective of treatment.[2,3]

PML is suspected in immune-compromised patients with progressive focal neurological deficits and characteristic neuroimaging studies.[1–3] The clinical presentation and imaging studies are nonspecific,[2,6,8] and definitive diagnosis has been dependent on pathological evaluation of brain tissue obtained by brain biopsy.[9] With no proven effective treatment, clinicians have been reluctant to subject patients to this procedure. JCV DNA in cerebrospinal fluid (CSF) identified by means of polymerase chain reaction (PCR) may have value in confirming the diagnosis.[9–12] Detection of JCV DNA in CSF has demonstrated a 74 to 92% sensitivity and a 92 to 100% specificity.[11,13–15] This level of specificity may be valuable for diagnosis and as an entry criterion for therapeutic trials. This report describes the strong relationship between clinical outcome and JCV DNA concentration in CSF. Our observations indicate that semiquantitative PCR is a significant diagnostic marker and an index of disease outcome.

Patients and Methods

Template Preparation

CSF samples were obtained from subjects participating in a study conducted by the AIDS Clinical Trials Group and the Neurologic AIDS Research Consortium. This protocol (ACTG 243) evaluated the safety and efficacy of intravenously and intrathecally administered cytosine arabinoside (Ara-c) in the treatment of HIV-infected patients with PML.[4]

Frozen CSF samples were received from participating sites. The usual sample volume was 1 ml, which was kept frozen until transferred to sterile microfuge tubes and centrifuged at 10,000 rpm for 2 minutes. CSF was removed and added to an equal volume of buffer-saturated phenol (BRL, Grand Island, NY; Life Technologies/Gibco), mixed, and extracted by repeated phenol/chloroform extraction. The sample was suspended in 20 μl of H_2O and divided into 8- and 12-μl aliquots.

PCR Amplification

Each template was serially diluted 10-fold to 10^{-1} and 10^{-2} for PCR amplification (Model 2400 Thermocycler; Perkin Elmer). The nucleotide sequence of primer 1 from the 5′ to 3′ orientation was from map position 4999 to 4979[16] GAA TAG GGA GGA ATC CAT GG; for primer 2, it was from map position 4231 to 4252 GGA ATG CAT GCA GAT CTA CAG G. These nucleotides are in the coding region for the viral early T protein, which is essential for virus growth. Amplification was initiated at 95°C for 30 seconds; performed for 40 cycles at 95°C for 30 seconds, 55°C for 30 seconds, and 72°C for 60 seconds; concluded with an extension cycle of 72°C for 7 minutes; and then held at 4°C.

Gel Analysis of PCR Products

Ten microliters of each PCR reaction product was electrophoresed through a 1.2% agarose gel in TBE (0.045 M of Tris, 0.045 M of boric acid, 0.001 M of EDTA; pH 7.4). Each gel contained eight samples: two CSF samples with three dilutions each as well as a negative control, no template control, and a positive control of 1 pg of JCV DNA amplified as described. They were submitted to Southern blot hybridization as described previously[17] using a ^{32}P-JCV DNA probe, which was normalized by disintegrations per minute so that hybridization of all CSF samples was done with the same activity of the probe. Autoradiographs were made on Kodak X-OMAT film (Eastman Kodak, Rochester, MN) at 24 and 120 hours. The amount of JCV DNA in the CSF sample was estimated from each gel by a comparison between the band intensity in the positive control and that of the bands in the samples and their dilutions by densitometric tracing (Molecular Dynamics, Sunnyvale CA). Analysis of the PCR reactions for each sample was done in duplicate by 4 laboratory members for a total of eight independent measurements. Under these conditions, there was no cross reac-

Fig 1. Southern blot hybridization of 10-fold serial dilutions of a JC virus (JCV) DNA template starting with 10 pg of DNA in lanes from left to right and ending with 0.01 fg. Estimation of the copy number of JCV DNA is based on the calculation that 1 pg of JCV DNA corresponds to 100,000 copies.

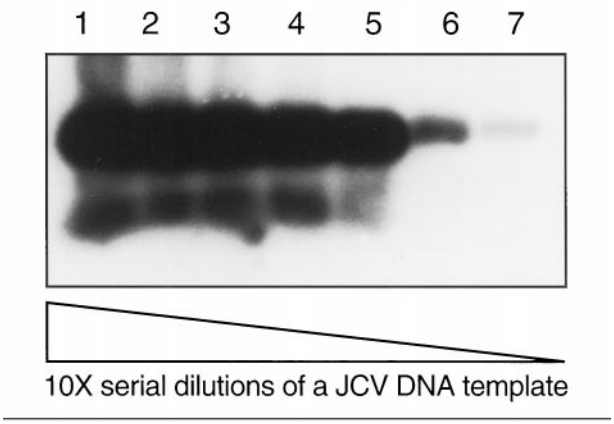

Table. Semiquantitative PCR Data (Viral Genome Copies per Microliter of CSF)

Patient Number	Study Week																	Survival (wk)	Weeks on Treatment
	2	3	4	5	6	7	8	9	10	11	12	13	14	16	18	20	22	24	
1		<0.1	<0.1	<0.1			<0.1		<0.1				<0.1						15.0	15.0
2	<0.1																		2.3	2.0
3	<0.1																		62.6[a]	1.6
4	<0.1	<0.1		<0.1	<0.1		<0.1		<0.1										33.7	17.1
5	3	3	10			5													8.3	7.3
6			30	30	<0.1		20		2				30	30					30.1	18.0
7	50	3	<0.1	3															17.9	6.9
8	60		8	2	10		10		<0.1		<0.1			2		1		2	47.0[a]	23.7
9	500	500	300																7.3	5.9
10	30	100	100	400	500														15.1	7.7
11	800		200	200															6.6	5.1
12	10	100	100																3.9	3.9
13	500	100																	16.9	2.9
14	50	70	30	30	70	70	100	<0.1											10.0[a]	8.6
15	60	70	50	150	70														7.9	5.9

Levels of JCV DNA below 0.1 copies/μl were undetectable. Subjects 1 through 4 constitute the *undetectable* JCV load group, subjects 5 through 8 constitute the *low* (intermediate) JCV load group, and subjects 9 through 15 constitute the *high* JCV load group.

[a]Patient was alive at the time of the last study visit.

tivity to either BK virus (BKV) or SV40 nucleotide sequences as previously described.[18]

The level of sensitivity of the PCR amplification method was determined by serial dilutions of JCV DNA starting with 10 pg to 0.01 fg and Southern blot hybridization to a radiolabeled probe. Figure 1 shows that the PCR protocol described previously followed by Southern blot hybridization could detect approximately 0.01 to 0.1 fg of DNA.

Collected Samples

CSF and plasma samples were obtained from subjects with biopsy-proven PML. Most subjects were treated with zidovudine alone or in combination with ddI, ddC and d4T. A small number received 3TC or protease inhibitors. CSF samples were collected from 15 subjects prior to intrathecal Ara-c administration on a weekly basis between weeks 3 and 6, biweekly during weeks 8 through 14, and every 4 weeks thereafter until the end of the study (week 26). Eleven subjects were male, and about half were white, with a median age of 38 years (range, 33–49 years). There was no association between demographics and JCV load at baseline. The median CD4 count was 29 cells/ml (range, 0–420 cells/ml) and was higher in subjects with undetectable versus detectable baseline JCV DNA (median, 107 vs 22 cells/ml; $p = 0.09$).

The PCR data set (viral genome copies/μl CSF) is presented in the Table along with duration of follow-up and treatment with Ara-C. Undetectable levels below 0.1 copies/μl are listed at the upper limit of assay sensitivity. Patient survival in subgroups, which is defined by presence or absence of JCV DNA and baseline JCV load, was compared by the log-rank test. the relationship between JCV load and survival was assessed by a Cox proportional hazards model that also included CD4 count.

Results

Eleven of 15 subjects had detectable baseline JCV DNA levels. The estimated sensitivity was 73.3%, which is close to reported estimates. Neither detection nor baseline JCV load was significantly associated with survival ($p = 0.49$ and 0.13, respectively). No subjects with undetectable JCV DNA developed detectable levels during the study, but previously detectable levels in 3 subjects fell below the level of detection.

Three subgroups were defined by their semiquantitative PCR profile: subjects with undetectable, low, and high JCV burden. Median survival was 24, 24.4, and 7.6 weeks, respectively ($p = 0.14$). Given the similarity of survival expectations, the undetectable and low groups were compared with the high group (Fig 2). Survival differences were statistically significant (median survival, 24 and 7.6 weeks, respectively; $p < 0.05$).

The impact of JCV load on survival was further elucidated by considering in a time-dependent fashion whether serial viral counts were above or below a cutoff point in a 50- to 100-genome copies/μl interval.* This interval, asserted by data inspection, has been confirmed through statistical analysis (data not shown) as the threshold maximally differentiating the two groups in terms of relative risk. JCV DNA levels above 50 to 100 copies/μl were strongly associated with increased mortality ($p < 0.01$). This effect was present in a multivariate model incorporating CD4 count, indicating

*We performed several analyses. In each case, a threshold between 50 and 100 genome copies/μl was chosen, and the data were recoded as: 0 = below the threshold, 1 = above the threshold. For example, if the chosen threshold value were 80 genome copies/μl, a value of 100 genome copies/μl would be recoded as 1, and a value of 30 genome copies/μl would be recoded as 0. As long as the threshold value was confined in the 50- to 100-genome copies/μl interval, the results were identical, and the resulting p values stayed in a narrow and statistically significant range ($p < 0.005$).

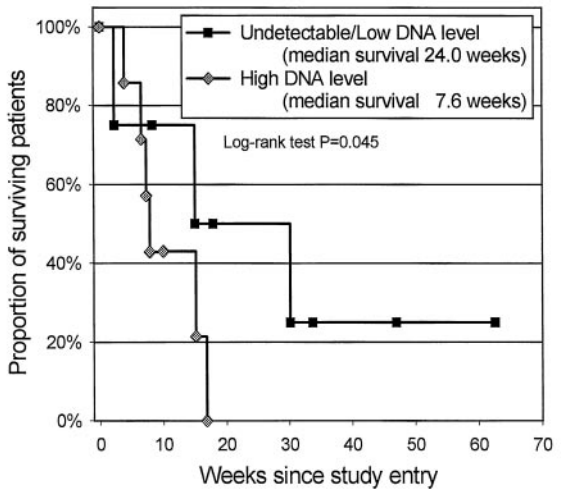

Fig 2. Patients with an undetectable or low JC virus (JCV) DNA concentration in the cerebrospinal fluid (median survival, 24 weeks) experienced longer survival compared with patients with a high viral DNA concentration (median survival, 7.6 weeks). The difference was statistically significant (log-rank, $p < 0.05$*).*

that CSF JCV burden is an informative marker beyond immunocompetence measures. Among PML patients with similar CD4 counts, those with a high JCV burden are at increased risk compared with those with a low or undetectable JCV load.

Fifty-three subjects provided 246 plasma samples collected every 4 weeks starting at baseline. Twelve of 52 baseline samples (23%) were JCV-positive, and 19 subjects (36%) had at least one positive on-study test. This proportion was no higher than that reported in the literature for the general HIV patient population with or without PML,[19] rendering detection of JCV DNA in plasma inappropriate for diagnostic purposes. In multivariate models that included CD4 counts, the presence of JCV DNA in plasma at baseline or during the study was not prognostic for patient survival. The chance of a positive test was inversely related to CD4 count.

Discussion

Detection of JCV DNA in plasma has no diagnostic significance and is likely a reflection of immunosuppression.[20] The proportion of positive tests remained within reported limits in the general population with advanced HIV disease. On the contrary, semiquantitation of JCV DNA concentration in CSF via PCR is a useful diagnostic aid, especially if a second test is performed after a negative test, as viral levels may transiently fall below the level of detection in patients with a low viral burden. Detection of PCR products using a ^{32}P-labeled JCV DNA probe following Southern blot hybridization increases the sensitivity and specificity of the assay. JCV and BKV share a 70% nucleotide similarity throughout their genomes, necessitating additional steps beyond identification of the PCR product following gel electrophoresis.

Low levels of JCV DNA are associated with longer patient survival. A threshold of 50 to 100 copies/μl separated high- from moderate-risk cases. JCV burden in the CSF supplements the information provided by CD4 count, implying that the PML disease course cannot simply be explained by changes in CD4. This observation is consistent with the findings of a recent study reporting only a weak correlation between CD4 counts and JCV burden in CSF.[20]

HIV viral load was not measured, and further research will determine whether knowledge of HIV burden would supersede the prognostic value of CSF JCV PCR. Nevertheless, recent studies report only partial success in treating PML with highly active antiretroviral therapy without full resolution of symptoms.[20] This would argue against HIV RNA changes fully accounting for the course of PML and that eradication of PML will likely depend on a combination of anti-retroviral and JC-specific therapy. Semiquantitative CSF JCV PCR may provide a reliable and relatively noninvasive prognostic marker of the effectiveness of these therapies.

This study was supported by grants PO1 NS3228, RR00036-37, RR00046, RR00051, RR00722, NS26643, AI-25903, A1-25868, AI-25915, and AI-38855 from the National Institutes of Health and by the AIDS Clinical Trials Group, National Institute of Allergy and Infectious Diseases.

Appendix

Participating Sites and Investigators

University of Kentucky School of Medicine, Lexington, KY (J. Berger); Veterans Affairs Medical Center, West Haven, CT (J. Booss); Beth Israel Deaconess Medical Center, Boston, MA (B. Dezube); Social and Scientific Systems, Rockville, MD (S. Shriver); Yale University School of Medicine, New Haven, CT (P. Jatlow); Albany Medical College, Albany, NY (S. Remick); Columbia-Presbyterian Medical College, New York, NY (M. Crawford, J. Dobkin, G. Dooneief, K. Marder); Johns Hopkins University, Baltimore, MD (R. Becker, K. Carter, A. Khan, V. Rexord); Massachusetts General Hospital and Harvard Medical School, Boston, MA (B. Navia, T. Flynn, M. Hirsch, E. McCarthy); Mount Sinai Medical Center, New York, NY (E. Chusid, P. Gerits, H. Mendoza, H. Sacks); Northwestern University, Evanston, IL (R. Levy, C. Cooper, R. Murphy, J. Phair); University of California, San Francisco, CA (S. Forstat, D. Gary, D. McGuire); University of Cincinnati, Cincinnati, OH; University of Colorado Health Sciences Center, Denver, CO (S. Canmann, K. Tyler); University Hospitals of Cleveland, Cleveland, OH (S. Weaver, S. Gordon); University of North Carolina, Chapel Hill, NC (K. Robertson, E. Atos Radzion, W. Robertson); University of Washington, Seattle, WA (C.

Marra, A. Collier, C. Cooper, J. Lund); Washington University School of Medicine, St Louis, MO (M. Glicksman, J. Voorhees, M. Royal).

References

1. Berger JR, Pall L, Lanska D, Whiteman M. Progressive multifocal leukoencephalopathy in patients with HIV infection. Journal of Neurovirology 1998;4:59–68
2. Berger JR, Concha M. Progressive multifocal leukoencephalopathy: the evolution of a disease once considered rare. Journal of Neurovirology 1995;1:5–18
3. Berger JR, Kaszovitz B, Post MJ, Dickinson G. Progressive multifocal leukoencephalopathy associated with human immunodeficiency virus infection. A review of the literature with a report of sixteen cases. Ann Intern Med 1987;107:78–87
4. Hall CD, Dafni U, Simpson D, et al. Failure of cytarabine in progressive multifocal leukoencephalopathy associated with human immunodeficiency virus infection. AIDS Clinical Trials Group 243 Team [see comments]. N Engl J Med 1998;338: 1345–1351
5. Karahalios D, Breit R, Dal Canto MC, Levy RM. Progressive multifocal leukoencephalopathy in patients with HIV infection: lack of impact of early diagnosis by stereotactic brain biopsy. J Acquir Immune Defic Syndr 1992;5:1030–1038
6. Berger JR, Levy RM, Flomenhoft D, Dobbs M. Predictive factors for prolonged survival in acquired immunodeficiency syndrome–associated progressive multifocal leukoencephalopathy. Ann Neurol 1998;44:341–349
7. Fong IW, Toma E. The natural history of progressive multifocal leukoencephalopathy in patients with AIDS. Canadian PML Study Group [see comments]. Clin Infect Dis 1995;20:1305–1310
8. Berger JR, Mucke L. Prolonged survival and partial recovery in AIDS-associated progressive multifocal leukoencephalopathy. Neurology 1988;38:1060–1065
9. Silver SA, Arthur RR, Erozan YS, et al. Diagnosis of progressive multifocal leukoencephalopathy by stereotactic brain biopsy utilizing immunohistochemistry and the polymerase chain reaction. Acta Cytol 1995;39:35–44
10. Weber T, Turner RW, Frye S, et al. Progressive multifocal leukoencephalopathy diagnosed by amplification of JC virus–specific DNA from cerebrospinal fluid. AIDS 1994;8:49–57
11. Weber T, Klapper PE, Cleator GM, et al. Polymerase chain reaction for detection of JC virus DNA in cerebrospinal fluid: a quality control study. European Union Concerted Action on Viral Meningitis and Encephalitis. J Virol Methods 1997;69: 231–237
12. Hammarin AL, Bogdanovic G, Svedhem V, et al. Analysis of PCR as a tool for detection of JC virus DNA in cerebrospinal fluid for diagnosis of progressive multifocal leukoencephalopathy. J Clin Microbiol 1996;34:2929–2932
13. Fong IW, Britton CB, Luinstra KE, Toma E, Mahony JB. Diagnostic value of detecting JC virus DNA in cerebrospinal fluid of patients with progressive multifocal leukoencephalopathy. J Clin Microbiol 1995;33:484–486
14. McGuire D, Barhite S, Hollander H, Miles M. JC virus DNA in cerebrospinal fluid of human immunodeficiency virus–infected patients: predictive value for progressive multifocal leukoencephalopathy [published erratum appears in Ann Neurol 1995;37:687]. Ann Neurol 1995;37:395–399
15. Weber T, Turner RW, Frye S, et al. Specific diagnosis of progressive multifocal leukoencephalopathy by polymerase chain reaction. J Infect Dis 1994;169:1138–1141
16. Frisque RJ, Bream GL, Cannella MT. Human polyomavirus JC virus genome. J Virol 1984;51:458–469
17. Monaco MC, Atwood WJ, Gravell M, et al. JC virus infection of hematopoietic progenitor cells, primary B lymphocytes, and tonsillar stromal cells: implications for viral latency. J Virol 1996;70:7004–7012
18. Grinnell BW, Padgett BL, Walker DL. Distribution of nonintegrated DNA from JC papovavirus in organs of patients with progressive multifocal leukoencephalopathy. J Infect Dis 1983; 147:669–675
19. Dubois V, Lafon ME, Ragnaud JM, et al. Detection of JC virus DNA in the peripheral blood leukocytes of HIV-infected patients. AIDS 1996;10:353–358
20. Koralnik IJ, Boden D, Mai VX, et al. JC virus DNA load in patients with and without progressive multifocal leukoencephalopathy. Neurology 1999;52:253–260

Exercise Intolerance due to a Nonsense Mutation in the mtDNA ND4 Gene

A. L. Andreu, MD,*† K. Tanji, MD,* C. Bruno, MD,*‡ G. M. Hadjigeorgiou, MD, PhD,* C. M. Sue, MD, PhD,* C. Jay, MD,§ T. Ohnishi, PhD,‖ S. Shanske, PhD,* E. Bonilla, MD,* and S. DiMauro, MD*

We report the first molecular defect in an NADH-dehydrogenase gene presenting as isolated myopathy. The proband had lifelong exercise intolerance but no weakness. A muscle biopsy showed cytochrome c oxidase (COX)–positive ragged-red fibers (RRFs), and analysis of the mitochondrial enzymes revealed complex I deficiency. Sequence analysis of the mitochondrial genes encoding the seven NADH-dehydrogenase subunits showed a G-to-A transition at nucleotide 11832 in the subunit 4 (ND4) gene, which changed an encoded tryptophan to a stop codon. The mutation was heteroplasmic (54%) in muscle DNA. Defects in mitochondrially encoded complex I subunits should be added to the differential diagnosis of mitochondrial myopathies.

Andreu AL, Tanji K, Bruno C, Hadjigeorgiou GM, Sue CM, Jay C, Ohnishi T, Shanske S, Bonilla E, DiMauro S. Exercise

From the *H. Houston Merritt Center for Muscular Dystrophy and Related Diseases, Department of Neurology, Columbia College of Physicians and Surgeons, New York, NY; †Centre d'Investigacions en Bioquimica i Biologia Molecular, Hospitals Vall d'Hebron, Barcelona, Spain; ‡Servizio Malattie Neuromuscolari, Department of Pediatrics, University of Genoa, Istituto Giannina Gaslini, Genoa, Italy; §University of California, San Francisco, Department of Neurology, San Francisco General Hospital, San Francisco, CA; and ‖Department of Biochemistry and Biophysics, University of Pennsylvania, Philadelphia, PA.

Received Jan 4, 1999. Accepted for publication Mar 5, 1999.

Address correspondence to Dr DiMauro, Department of Neurology, 4-420 College of Physicians and Surgeons, 630 West 168th Street, New York, NY 10032.

intolerance due to a nonsense mutation
in the mtDNA ND4 gene.
Ann Neurol 1999;45:820–823

Mitochondrial DNA (mtDNA) mutations have been associated with a wide range of clinical presentations ranging from pure myopathies to multisystemic disorders. Most of these mutations were in transfer RNA (tRNA) genes, but increasing number of mutations are being reported in polypeptide-coding genes.[1] Here, we present a nonsense mutation in the mtDNA gene encoding subunit 4 of NADH dehydrogenase (ND4) in a patient with pure myopathy and complex I deficiency. This is the first mutation in a complex I gene to be associated with myopathy and the first nonsense mutation to be reported in a complex I gene.

Material and Methods

Case Report

A 38-year-old man complained of lifelong exercise intolerance. He described premature fatigue and myalgia even after moderate exercise such as walking on level ground for 20 minutes. Walking uphill or upstairs is an activity that he can only tolerate for a few minutes. If he forces himself to exercise, he feels exhausted on the following day, and the muscles he has used feel sore. He has never noticed pigmenturia. He believes his legs are more affected than his arms. A cardiovascular consultation revealed no cardiac dysfunction. The neurological examination was normal, including muscle bulk and strength. Resting serum creatine kinase was normal. Lactic acid was 5.2 mEq/L (normal values, 0.5–2.2 mEq/L) and rose excessively after a standardized aerobic exercise (9.2 mEq/L after 1 minute). Electromyographic (EMG) findings were normal. His family history was negative for neuromuscular disorders; specifically, his mother and 2 sisters do not complain of exercise intolerance.

Biochemical Studies

Biochemical analysis of mitochondrial enzymes in muscle homogenates showed an isolated defect of complex I activity (Table), which was even more pronounced when referred to the activity of citrate synthase, which is a matrix enzyme and a good marker of mitochondrial "mass."

Histochemistry

Muscle frozen sections of 6-μm thickness were stained histochemically with succinate dehydrogenase and cytochrome c oxidase (COX) according to described methods.[2] Succinate dehydrogenase staining showed scattered ragged-red fibers (RRFs), which stained intensely for COX activity and contained an increased number of lipid droplets (Fig, A). No COX-negative fibers were seen. Single-fiber analysis performed by described methods[3] showed that the mutation was much more abundant in RRFs than in non-RRFs (92.4 ± 1.95% vs 12.4 ± 7.3%) (see Fig, B).

Molecular Genetic Studies

Muscle DNA was extracted according to conventional methods, and 12 polymerase chain reaction (PCR) products overlapping the entire coding region for the seven NADH-dehydrogenase subunits were obtained using the set of primers previously reported for sequencing the entire mitochondrial genome.[4] Direct sequencing of PCR products was performed using the same set of primers (forward and reverse) in an automatic sequencer (Model 310 Automatic Sequencer; Perkin Elmer, Foster City, CA). Sequence analysis of the PCR products showed 15 nucleotide changes compared with the Cambridge sequence.[5] Fourteen were either known errors in the reference sequence or neutral polymorphisms. The 15th change was a G-to-A transition at nucleotide position 11832 in the ND4 gene (see Fig, C), which caused the substitution of tryptophan-358 (UGA) with a stop codon (UAA) and resulted in the loss of 102 amino acids from the C terminus of the ND4 subunit equivalent to 22% of the total polypeptide length. To quantitate the proportion of mutant mtDNA, we performed PCR–restriction fragment-length polymorphism (RFLP) analysis. A 286-base pair fragment was amplified using the following primers: 21-mer forward (5′-cagtcatt-ctcataatcgccc-3′) and 20-mer reverse (5′-ggagtatagggctgtgacta-3′). α-P^{32} deoxyadenosine triphosphate was added in the last PCR cycle to avoid underestimation of the mutated mtDNA molecules due to heteroduplex formation. Because the mutation creates a novel restriction site for *Mse*I, this enzyme was used for RFLP analysis. Digested PCR products were run through a 12% nondenaturing polyacrylamide gel and subjected to autoradiography. RFLP analysis showed that the mutation was heteroplasmic in the patient's muscle (54%) but that it was not detectable in blood (see Fig, C). Using PCR-RFLP analysis of DNA isolated from muscle, we could not detect this mutation

Table. Mitochondrial Enzyme Activities in the Patient's Muscle

	Controls[a]	Patient[b]
NADH–cytochrome c reductase (I + III)	1.02 ± 0.52	0.54 (53)
NADH dehydrogenase (I)	35.5 ± 7.07	9.91 (28)
Succinate–cytochrome c reductase (II + III)	0.70 ± 0.23	0.76 (109)
Succinate dehydrogenase (II)	1.00 ± 0.53	1.63 (163)
Cytochrome c oxidase (IV)	2.80 ± 0.52	3.83 (137)
Citrate synthase	9.88 ± 2.55	17.9 (181)

[a]Values are expressed as micromoles per minute per gram. Control values are mean ± SD in 20 individuals.
[b]Numbers in parentheses are percentages of the mean normal values.

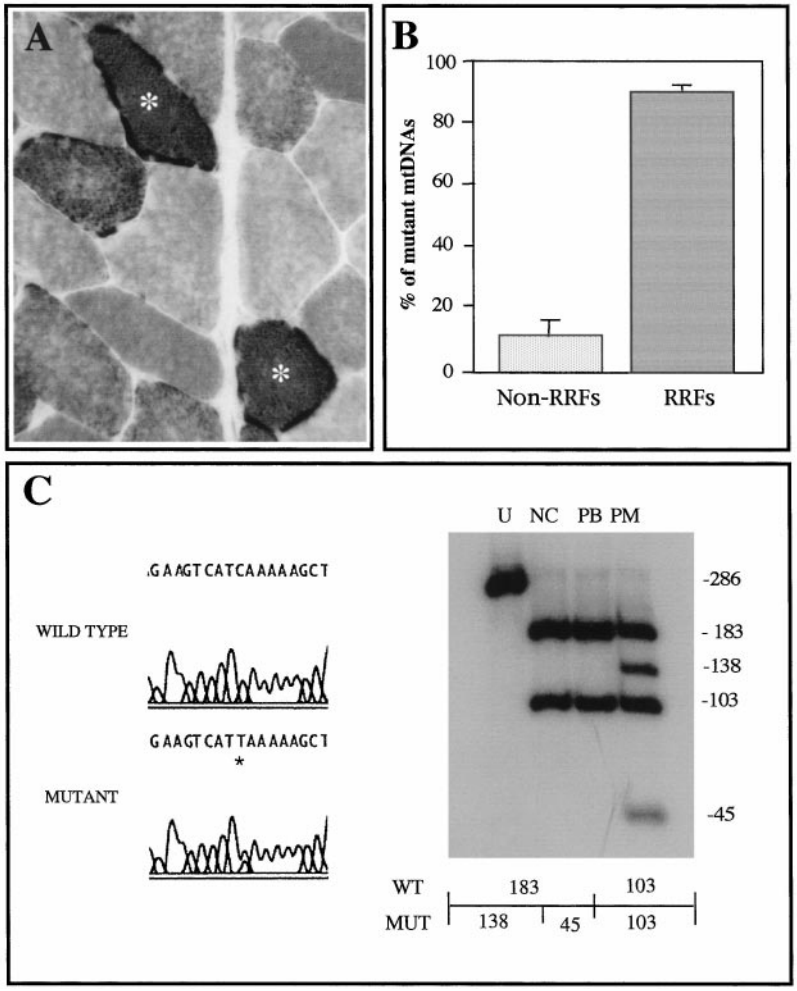

Fig. (A) Cytochrome c oxidase (COX) staining in the patient's muscle. Asterisks *indicate COX-positive ragged-red fibers (RRFs). (B) Percentage of mutated mtDNA in non-RRFs and RRFs is demonstrated by means of single-fiber polymerase chain reaction analysis. (C) Left: Electropherogram of ND4 gene showing the sequence of muscle DNA in a control and in the patient. Sequencing was performed using a reverse primer and shows the G11832A transition (C-to-T transition in the reverse sequence). Right: Restriction fragment-length polymorphism analysis.* Mse*I cuts the original fragment (286 bp) into two fragments of 183 and 103 bp. The mutation creates a new restriction site for* Mse*I that cuts the 183-bp fragment into two fragments of 138 and 45 bp. U = uncut fragment; NC = normal control muscle; PB = patient's blood; PM = patient's muscle.*

in 100 controls (40 normal individuals and 60 patients with different pathogenic mtDNA mutations).

Discussion

This patient complained of lifelong exercise intolerance but had no fixed weakness, and both neurological examination and EMG findings were normal. It is fair to assume that such subjective complaints would be easily dismissed even by competent neurologists as "psychogenic." Nevertheless, an increased level of blood lactate, which was even more pronounced after aerobic exercise on a treadmill, suggested mitochondrial dysfunction and led to a muscle biopsy. The finding of COX-positive RRFs and decreased complex I activity prompted us to sequence the seven mtDNA genes encoding complex I subunits. We found a nonsense mutation in the ND4 gene. This is the first mutation in a complex I subunit gene to be associated with pure myopathy and the first nonsense mutation to be detected in a complex I gene. Evidence supporting the pathogenicity of this mutation includes the following findings:

1. Heteroplasmy was detected in muscle (54%), which is typical for pathogenic mtDNA mutations. Moreover, the lack of the mutation in blood, the absence of multisystemic involvement, and the lack of maternal inheritance suggest that this mutation may have arisen de novo during embryogenesis and may not be present in the germ line. This concept is in agreement with recent findings in patients with myopathy harboring mutations in the cytochrome b gene, in whom the molecular defect was also confined to muscle and was not present in maternal relatives.[6–9]
2. The mutation is consistent with the biochemical defect of isolated complex I deficiency in muscle.
3. This nonsense mutation causes the loss of 102 amino acids from the C terminus of the polypeptide, which undoubtedly impairs the function of complex I.
4. Single-fiber analysis showed a clear relationship between the abundance of the mutation and morphological alterations.

Until recently, mutations in mtDNA associated with isolated myopathy had been in tRNA genes: T3250C and A3302G in $tRNA^{Leu(UUR)}$,[10,11] A12320G in $tRNA^{Leu(CUN)}$,[12] and C15990T in $tRNA^{Pro}$.[13] Recently, however, several mutations in protein-encoding genes have been observed in patients with selective muscle involvement. These include a microdeletion in the gene encoding COX III[14] and four distinct mutations in the cytochrome b gene.[6–9] Interestingly, all of these cases have been sporadic. Mutations in NADH-dehydrogenase genes have been mostly associated with Leber's hereditary optic neuropathy, including the first point mutation identified in mtDNA, G11778A in the ND4 gene.[15] Besides "primary" and "secondary" Leber's hereditary optic neuropathy mutations, two mutations, one in the ND1 gene and the other in the ND5 gene, have recently been described in 2 patients with the mitochondrial encephalomyopathy, lactic acidosis, and stroke-like episodes syndrome (MELAS).[16,17] Unlike the mutation described here, those mutations were missense, multisystemic, and maternally inherited.

In conclusion, mutations in protein-encoding genes of mtDNA should be carefully considered in the differential diagnosis of sporadic patients with exercise intolerance even when neurological examination and EMG findings are normal as in the case presented in this report.

This study was supported by the Muscular Dystrophy Association and NIH grants PO1HD32062 and NS11766 (S.D.), the Fondo de Investigationes Sanitarias BAE 98/5144 (A.L.A.), and Telethon-Italy (C.B.).

References

1. DiMauro S, Bonilla E. Mitochondrial encephalomyopathies. In: Rosenberg RN, Prusiner SB, DiMauro S, Barchi RL, eds. The molecular and genetic basis of neurological disease, 2nd ed. Boston: Butterworth-Heinemann, 1997:201–235
2. Sciacco M, Bonilla E. Cytochemistry and immunocytochemistry of mitochondria in muscle sections. In: Attardi GM, Chomyn A, eds. Methods in enzymology. San Diego: Academic Press, 1996:509–521
3. Sciacco M, Bonilla E, Schon EA, et al. Distribution of deleted and wild-type mtDNA in normal and respiration-deficient muscle fibers from patients with mitochondrial myopathy. Hum Mol Genet 1994;3:13–19
4. Rieder MJ, Taylor SL, Tobe Vo, Nickerson DA. Automatic identification of DNA variations using quality-based fluorescence re-sequencing: analysis of the human mitochondrial genome. Nucleic Acids Res 1998;26:967–973
5. Anderson S, Bankier AT, Barrell BG, et al. Sequence and organization of the human mitochondrial genome. Nature 1980; 290:457–465
6. Dumoulin R, Sagnol I, Ferlin T, et al. A novel gly290asp mitochondrial cytochrome b mutation linked to a complex III deficiency in progressive exercise intolerance. Mol Cell Probes 1996;10:389–391
7. Kennaway NG, Keightley JA, Burton MD, et al. Mitochondrial encephalomyopathy associated with a nonsense mutation in the cytochrome b gene. Molec Genet Metab 1998;63:49 (Abstract)
8. Andreu AL, Bruno C, Shanske S, et al. Missense mutation in the mtDNA cytochrome b gene in a patient with myopathy. Neurology 1998;51:1444–1447
9. Andreu AL, Bruno C, Dunne TC, et al. A nonsense mutation (G15059A) in the cytochrome *b* gene in a patient with exercise intolerance and myoglobinuria. Ann Neurol 1999;45:127–130
10. Goto Y, Tojo M, Tahyama J, et al. A novel point mutation in the mitochondrial tRNA(leu)(UUR) gene in a family with mitochondrial myopathy. Ann Neurol 1992;31:672–675
11. Bindoff LA, Howell N, Poulton J, et al. Abnormal RNA processing associated with a novel tRNA mutation in mitochondrial DNA. A potential disease mechanism. J Biol Chem 1993; 268:19559–19564
12. Weber K, Wilson JN, Taylor L, et al. A new mtDNA mutation showing accumulation with time and restriction to skeletal muscle. Am J Hum Genet 1997;60:373–380
13. Moraes CT, Ciacci F, Bonilla E, et al. A mitochondrial cRNA anticodon swap associated with a muscle disease. Nat Genet 1993;4:284–289
14. Keightley JA, Hoffbuhr KC, Burton MD, et al. A microdeletion in cytochrome c oxidase (COX) subunit III associated with COX deficiency and recurrent myoglobinuria. Nat Genet 1996; 12:410–416
15. Wallace DC, Singh G, Lott MT, et al. Mitochondrial DNA mutation associated with Leber's hereditary optic neuropathy. Science 1988;242:1427–1430
16. Santorelli F, Tanji K, Kulikova R, et al. Identification of a novel mutation in the mtDNA ND5 gene associated with MELAS. Biochem Biophys Res Commun 1997;238:326–328
17. Campos Y, Martin MA, Rubio JC, et al. Bilateral striatal necrosis and MELAS associated with a new T3308C mutation in the mitochondrial ND1 gene. Biochem Biophys Res Commun 1997;238:323–325

Correction

In the article "Miller Fisher anti-GQ1b antibodies: α-latrotoxin–like effects on motor end plates" by Plomp et al in the February issue (Ann Neurol 1999; 45:189–199), the title of the table on page 191 was a misprint. The correct title is as follows:

Table. Effects of MFS Sera and Purified IgG on Mouse Diaphragm

The publisher apologizes for the error.